PEOPLE'S DEMOCRATIC REPUBLIC OF ALGERIA

Ministry of Higher Education and Scientific Research

University of Blida 1

Faculty of Technology

Department of Process Engineering

Thesis

In partial fulfillment of the requirements for the degree of

MASTER IN PROCESS ENGINEERING

Specialty: Pharmaceutical industry

Thesis Title**:**

Synthesis of zinc oxide nanoparticles, evaluation of their antimicrobial activity and transdermal diffusion via a hydrogel matrix.

Presented by:

-BAYOU Salima

-TAOUG Ferial

Supervised by:

- Dr. M. REBIHA

- Ph.D. Student S. HABET

Class of 2025

Résumé

L'objectif de ce travail est le développement d'un hydrogel à base de Carbopol incorporant des nanoparticules d'oxyde de zinc (ZnO), à visée antimicrobienne et transdermique. Cinq formulations d'hydrogel ont été préparées avec des concentrations croissantes de Carbopol (de 0,2 % à 0,6 %). Après étude rhéologique, la formulation optimale a été retenue à 0,3 %. Les nanoparticules de ZnO ont été synthétisées par précipitation, puis caractérisées par UV-Visible, diffraction des rayons X (XRD), infrarouge (FTIR), diffusion dynamique de la lumière (DLS) et potentiel zêta. L'hydrogel final contenant les ZnO a été évalué par spectroscopie infrarouge, mesure du pH, analyse rhéologique, test de diffusion transdermique (cellule de Franz), ainsi que des tests d'activité antibactérienne et antifongique. Les résultats ont révélé une bonne stabilité de la formulation, une viscosité appropriée, un profil de libération transdermique régulier, et une activité antibactérienne notable. Une activité antifongique modérée a été observée, limitée à une levure, suggérant un potentiel à explorer davantage.

Mots-clés : Hydrogel, nanoparticules oxyde de zinc, caractérisation, diffusion transdermique, activité antimicrobienne.

Abstract

The aim of this work is to develop a Carbopol-based hydrogel incorporating zinc oxide nanoparticles (ZnO NPs) for antimicrobial and transdermal applications. Five hydrogel formulations were prepared using increasing concentrations of Carbopol (from 0.2% to 0.6%). Based on rheological evaluation, the optimal formulation was selected at 0.3%. ZnO nanoparticles were synthesized via precipitation and characterized using UV-Visible spectroscopy, X-ray diffraction (XRD), Fourier-transform infrared spectroscopy (FTIR), dynamic light scattering (DLS), and zeta potential analysis. The final ZnO-loaded hydrogel was characterized by FTIR, pH measurement, rheological testing, transdermal diffusion study (Franz cell), and antibacterial and antifungal activity assays. The results showed good formulation stability, suitable viscosity, a consistent transdermal release profile, and notable antibacterial efficacy. A moderate antifungal activity was observed, limited to one yeast strain, indicating potential for further investigation.

Keywords: Hydrogel, zinc oxide nanoparticles, characterization, transdermal diffusion, antimicrobial activity.

الملخص

يهدف هذا البحث إلى تطوير هيدروجيل قائم على الكاربوبول يحتوي على جسيمات نانوية من أكسيد الزنك للاستخدام الموضعي وعبر الجلد كمضاد للميكروبات. تم تحضير خمس تركيبات من الهيدروجيل بتركيزات متزايدة من الكاربوبول (من 0.2٪ إلى 0.6٪). وبناءً على تحليل السلوك الريولوجي، تم اختيار التركيبة المثلى بتركيز 0.3٪ .تم تصنيع جسيمات ZnO النانوية عن طريق طريقة الترسيب، وتم توصيفها باستخدام التحليل الطيفي بالأشعة فوق البنفسجية والمرئية(UV–Vis) ، وحيود الأشعة السينية(XRD) ، ومطيافية الأشعة تحت الحمراء(FTIR) ، وتحليل التشتت الديناميكي للضوء(DLS) ، وتحليل الجهد السطحي .(ζ) تم تقييم الهيدروجيل النهائي المحتوي على ZnO بواسطةFTIR ، وقياس الرقم الهيدروجيني(pH) ، والاختبارات الريولوجية، واختبار الانتشار عبر الجلد (خلية فرانز)، بالإضافة إلى اختبارات النشاط المضاد للبكتيريا والفطريات .أظهرت النتائج أن التركيبة مستقرة، ولها لزوجة مناسبة، وملف إطلاق متوازن عبر الجلد، وفعالية ملحوظة ضد البكتيريا. كما لوحظ نشاط مضاد للفطريات متوسط، اقتصر على نوع واحد من الخمائر، مما يشير إلى إمكانية التوسع في الدراسة لاحقا.

الكلمات المفتاحية: الهيدروجيل، جسيمات أكسيد الزنك النانوية، التوصيف، الانتشار عبر الجلد، النشاط المضاد للميكروبات

Acknowledgements

First and foremost, we would like to thank **Allah**, the Almighty, for granting us the will, patience, and health throughout these years of study.

We also express our deep gratitude to our parents for their love, sacrifices, unconditional support, and constant encouragement.

Our sincere thanks go to Dr. Rebiha, our supervisor, for her availability, understanding, encouragement, and the trust she placed in us throughout this work. We extend to her our utmost respect and heartfelt appreciation.

We are also deeply grateful to Professor Hadj Ziane for her invaluable guidance, and in particular for her assistance with the DLS and zeta potential analyses, as well as for generously granting us access to her laboratory when needed.

We warmly thank Mrs. Rachida, laboratory engineer,

for her invaluable help, patience, and daily availability. She supported us with great professionalism throughout the experimental stage.

Our sincere appreciation goes to PhD student Habet Sara for her assistance with the transdermal diffusion tests, as well as to Mrs. Ayachi and her student Loubna whose help was essential during the antimicrobial activity study. Thanks to them, we were able to obtain the necessary strains and carry out the tests under good conditions.

We would also like to express our sincere gratitude to all the members of the LAFPC laboratory, as well as its president, Prof. Hadj Sadouk, for their invaluable support and for kindly granting us access to their facilities.

We would also like to thank PhD student Abir for conducting the antibacterial activity tests, and Professor Zermane for professionally handling the XRD analysis.

Finally, we express our gratitude to the jury members for the interest they have shown in our work, and to all those who, directly or indirectly,

contributed to the success of this project.

Dedication

First and foremost, I express my deepest gratitude to God, for granting me the will, the strength both mental and physical and the perseverance to reach this milestone.

This work is lovingly dedicated to my light at the end of the tunnel, my greatest joy, my hero the strongest woman I have ever known, even in the face of unimaginable loss of my grandmother, my mommy. This one is for you.

To my father, who could not be here today, and who has been courageously fighting for his life over the past six months I hope this achievement brings a little light to your heart. I am always praying of you.

To my brothers, Ahmed who was always there for me in every step I took for being so supportive and understanding, Amir, and Fares my warriors thank you for being the shoulders I could lean on when I needed strength.

To my sister Narimane, my confidant even when you joked that I spent all my time studying and not enough with you, know that your presence and support meant everything to me.

To my sisters-in-law, Imane and Soumia your kindness, encouragement, and help through the tough times, especially with this thesis, will never be forgotten.

To my beloved nieces, Céline, Anaïs, and Dina my princesses, my joy and to my nephew Djawed, my little prince, your smiles made everything brighter.

To my aunt Samira, my second mother, and her three beautiful children thank you for being a constant source of comfort and care and help.

To my best friend Fella, thank you for always being there for me, listening to me vent again and again, reminding me of my strength, and encouraging me every single time.

To my comrade Salima, thank you for being by my side during this amazing journey. Together we learned teamwork, resilience, and built a lasting friendship. We really did something incredible.

And last but not least, I want to thank me.

I want to thank me:

For believing in myself.

For not giving up.

For trying harder every single time.

And for always coming back stronger.

FERIAL TAOUG

Dedication

This thesis is more than just an academic requirement. It is the reflection of a journey filled with perseverance, emotions, and the invaluable support of those who walked by my side.

To my mother, Thank you for your endless love, your prayers whispered in silence, your warm hugs, and your gentle strength. You have been my greatest comfort, my light during hard times, and my constant support. I owe so much to your unwavering presence.

To my father, Thank you for believing in me even when I doubted myself, for your sacrifices, your wise advice, and your quiet encouragement. Your strength, discipline, and love have shaped who I am today. I am proud to be your daughter.

To my sister Serine and my brothers Akram & Nassim, Thank you for your constant support, your comforting presence, and your sincere encouragement. Your smiles and words gave me strength through every challenge

I am deeply thankful to have you in my life.

To Ferial, my comrade and binôme, Thank you for being more than a lab partner. Through shared efforts, pressure, and success, we've built a friendship that I truly value. Your support and presence throughout this journey made the experience even more meaningful.

To my dear friends Tesnim, Maria, Ryma, and Amira, Thank you for your friendship, your kindness, your uplifting words, and the laughter we shared. Your presence has made this journey lighter, brighter, and more beautiful. You've been my rays of sunshine during this academic marathon.

A special thanks to Maria, My loyal and precious friend who stood by me every step of the way. Thank you for being present during the research, the long discussions, and especially during moments of stress and fatigue. Your constant support, patience, and sincere dedication have meant the world to me.

And above all, I want to thank me. For holding on through the hard days. For keeping my heart soft, my mind open, and my spirit strong. For staying kind even when it was hard. For carrying the weight of pressure with grace.

I didn't just survive this I grew through it.

SALIMA BAYOU

TABLE OF CONTENTS

Figures List

Tables List

Abbreviations List

AMR : Antimicrobial Resistance

CNO : Cyanate ion

CNTs : Carbon Nanotubes

DNA : Deoxyribonucleic Acid

DLS : Dynamic Light Scattering

FTIR : Fourier Transform Infrared Spectroscopy

g : Gram

G' : Storage Modulus

G" : Loss Modulus

JCPDS : Joint Committee on Powder Diffraction Standards

LiOH : Lithium Hydroxide

log K : Logarithm of the Equilibrium Constant

L : Liter

LVR : Linear Viscoelastic Region

mol : Mole

mPa·s : Millipascal Second (viscosity unit)

NaOH : Sodium Hydroxide

NH_4OH : Ammonium Hydroxide

NPs : NanoParticules

OH^- : Hydroxide Ion

PDI : Polydispersity Index

PEG : Polyethylene Glycol

PVP : Polyvinylpyrrolidone

pH : Hydrogen Potential

ROS : Reactive Oxygen Species

SC : Scandium

TG : Thermogravimetric Analysis

UV-Vis : Ultraviolet–Visible Spectroscopy

XRD : X-ray Diffraction

Zn^{2+} : Zinc Ion

$Zn(CH_3COO)_2 \cdot 2H_2O$: Zinc Acetate Dihydrate

$Zn(NO_3)_2 \cdot 6H_2O$: Zinc Nitrate Hexahydrate

$Zn(OH)_2$: Zinc Hydroxide

ZnO NPs : Zinc Oxide Nanoparticles

$ZnSO_4 \cdot 7H_2O$: Zinc Sulfate Heptahydrate

°C : Degree Celsius

GENERAL INTRODUCTION

GENERAL INTRODUCTION

Zinc oxide nanoparticles (ZnO-NPs) have attracted a great deal of interest because of their novel physicochemical properties such as large surface area to volume ratio, semiconducting nature, as well as excellent antimicrobial activity [1]. These characteristics render ZnO-NPs quite interesting for pharmaceutical and cosmetic formulations, particularly in topical gels with an antibacterial purpose [2].

An emerging menace due to the occurrence of antimicrobial resistance (AMR) demand for a new and novel antibacterial agent [3]. ZnO-NPs have exhibited potent antibacterial and antifungal activities through various actions such ROS production, Zn^{2+} release, and direct contact with microbial cell walls [4]. These effects make ZnO-NPs prospects to incorporate in topical gels for the prevention or treatment of skin infections [5].

ZnO-NPs can be produced by different techniques such as physical, chemical, and biological (green synthesis).

The ZnO-NPs antimicrobial activity is highly affected by synthesis parameters, such as the particle size, surface charge, and shape [6]. Smaller NPs normally show more antibacterial performance because of higher surface reactivity and ROS generation as pointed out [7].

The use of ZnO-NPs as an additive in gels / hydrogels has the potential to improve the stability, rheological features, and therapeutic efficacy of gels/hydrogels [8]. ZnO-NPs have been found to affect gel viscosity, drug solubility and diffusion kinetics, which can be helpful in the design of antibacterial and transdermal drug delivery products [9].

Compared to the conventional topical applications, transdermal drug delivery has several advantages such as slow drug release, better drug permeation, and lower systemic side effects [10].

However, effective transdermal formulations require penetration enhancers to facilitate drug diffusion across the skin barrier. ZnO-NPs have been investigated for their ability to modulate transdermal diffusion, either by interacting with the stratum corneum or by altering the microenvironment of the gel [11].

GENERAL INTRODUCTION

This document is organized into two main parts. The first part is dedicated to a literature review on the formulation of ZnO-based hydrogels, their properties, antibacterial activities, and transdermal diffusion. The experimental part of this work is presented in Chapters Three and Four.

The third chapter focuses on the synthesis of ZnO nanoparticles, the formulation of hydrogels, and their incorporation. We present the experimental procedure as well as the characterization techniques such as FT-IR, XRD, DLS, zeta potential, UV-Vis spectroscopy, and rheological study, along with the methods for evaluating antibacterial effects and transdermal diffusion.

The fourth chapter is based on the discussion of the results obtained from the samples, along with the interpretation of each result.

Finally, a conclusion, which is the last part of this work, presents the main results achieved as well as the possible directions for further in-depth studies.

CHAPTER I:

ZINC OXIDE NANOPARTICLES

CHAPTER I: ZINC OXIDE NANOPARTICLES

In 1959, American physicist and Nobel Laureate Richard Feynman said, "There's Plenty of Room at the Bottom," which opened the new field of nanotechnology. The concept of “nanotechnology” was first suggested 15 years after by Professor Norio Taniguchi that he proposed in the 1974 paper ‘Nano-technology’ that mainly consists of the processing of, separation, consolidation, and deformation of materials by one atom or by one molecule” [12].

I.1. Nanoparticles:

NPs come in all shapes, sizes and forms. [13] They may be spherical, cylindrical, spiral, etc., or irregular.

I.1.1. Definition of Nanoparticles:

NPs can range in size from 1 to 100 nm. NPs may be crystalline, with single or multicrystal solids, or amorphous. NPs can have either a loose or an agglomerated characteristic [14]. Those nanoparticles can be sorted by numerous criterion such as their origin, chemistry, size, properties and use. [15]; In addition, nanoparticles are generally classified organic (polymer, lipid, DNA, protein, etc.) and inorganic, (metallic, metal oxides, ceramic, etc.). [16]

I.1.2. Classification of Nanoparticles:

According to the material that formed the nanostructure, NPs are commonly classified in three groups: organic, carbon based, and inorganic.

I.1.2.1. Carbon based NPs:

This category consists of NPs constructed entirely of carbon atoms. Well known material in this class includes fullerenes, carbon black NPs, and carbon quantum dots [17].

I.1.2.2. Organic NPs:

This category includes all NPs, which are composed of proteins, carbohydrates, lipids, polymers, or other types of organic compounds [18]. Notable members of this class include dendrimers, liposomes, micelles, and protein complexes like ferritin [17].

I.1.2.3. Inorganic NPs:

Inorganic nanoparticles are those that do not contain atoms of carbon. In most of the cases, inorganic nanoparticles are referred to as being composed of metals or metal oxides.

a) Metal-Based Nanoparticles:

Nanoparticles can be manufactured destructively or their synthesis involves the building-up method: aluminium, cadmium, cobalt, copper, gold, iron, lead, silver, and zinc are some of the metals that are frequently used in nanoparticle creation. Owing to very good optical features, metal nanomaterials are applied in several research fields. [19]

b) Metal oxide Nanoparticles:

The inorganic metal oxide nanoparticles, in simple words, are the nanomaterials of metal oxides and mostly the combination of the positive metallic ion with the negative one of oxygen. Examples of metal oxide nanoparticles include silicon dioxide (SiO_2), titanium oxide (TiO_2), zinc oxide (ZnO), and aluminium oxide (Al_2O_3). These nanoparticles exhibit fairly remarkable properties when compared to their metal analog. [19]

I.2. Zinc Oxide Nanoparticles (ZnO NPs)

Zinc oxide nanoparticles, abbreviated as ZnO NPs, are one of the most interesting and promising metallic nanomaterials arising from zinc oxide. It is also an active member and at the same time a very strong reducing agent, implying that it can easily be oxidized to form ZnO according to the potential of reduction [20].

I.2.1. Definition of ZnO

Contrary to this, zinc oxide nanoparticles gained distinct attention in designing the second generation of nanoantibiotics against pathogenic microorganisms that work in facing multidrug resistance. The above special physicochemical properties of these NPs were assessed based on morphological parameters, particle size, crystallinity, or porosity. With that being well established for its many attributes, ZnO NPs offer a high array of antimicrobial activities toward microorganisms composed mainly of Escherichia coli, Staphylococcus aureus, Pseudomonas aeruginosa [24–25].

I.2.2. Characteristics of ZnO Materials Based on Synthesis Techniques:

ZnO NPs (81.38 g/mol, <100 nm) are white and odourless solid hexagonal wurtzite crystals, representing a wide variety of shapes such as spheres in zero-dimensional structures, dumbbells, nanorods, and nanotubes and needles in one-dimensional structures, disks and platelets for two-dimensional structures, and flowers, stars, and flakes for three-dimensional structures [26].

Most of the physicochemical properties of ZnO materials lie in the antimicrobial potential against pathogenic microorganisms because health responses are related to pharmacological and toxicological parameters [27].

It is due to these properties that morphology, particle size, and porosity of metal oxide NPs confer superior antimicrobial activity against pathogenic microorganisms. The relevant physicochemical properties of ZnO NPs/MPs depend on the synthesis techniques applied during their preparation [28, 26, 29].

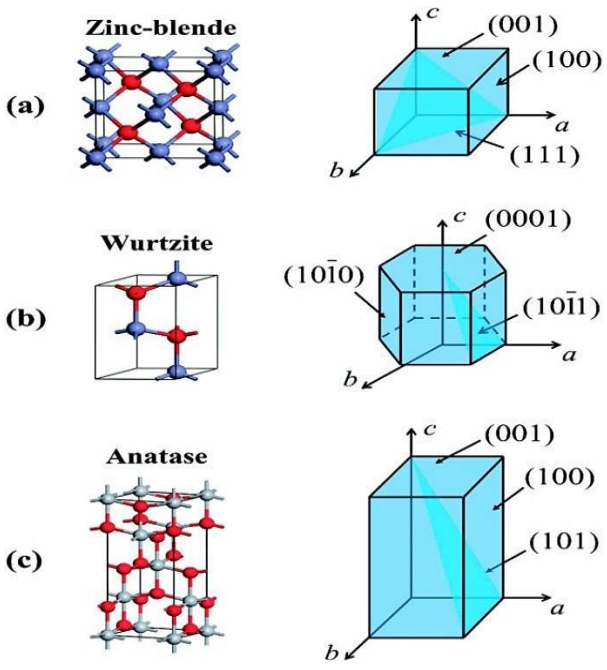

Figure I.1: Different structures of Zinc oxide [26].

Zinc oxide is known for its unique optical, chemical sensing, semiconducting, electric conductive, and piezoelectric properties. [29] The material exhibits a direct wide band gap at 3.3 eV for near UV, high excitonic binding room temperature energy at 60 meV, and natural n-type electrical conductivity. [30]

ZnO can present different growth morphology including nanocombs, nanorings, nanohelixes, nanobelts, nanowires and nanocages [29, 30].

I.3. Synthesis Methods of ZnO NPs:

The methods that are applied towards the synthesis of nanomaterials are generally two types: bottom-up strategies and top-down strategies.

I.3.1. Top-down Approach:

The top-down means used benefit from the implementation of a variety of technologies for the production of small structures from large ones, such as ultrasonic treatment, laser ablation, mechanical milling, and vapor deposition. This process has a variety of limitations which includes time-consumption and expensive to develop which results in difficulties to formulate nanoparticles. [31]

I.3.2. Bottom-up Approach:

The production of metal nanoparticles from metal precursors in solid, liquid, or gas phases defines the bottom-up processes. These procedures are known as the bottom-up chemical processes, encompassing sol-gel processing, chemical co-precipitation, and chemical vapor deposition, typically ending in toxic by-products. The bottom-up methods can be generally outlined into two categories: in principle and by definition, the bottom-up methods are dominated by conventional methods for NP synthesis, such as physical, chemical, and biological ones. [32]

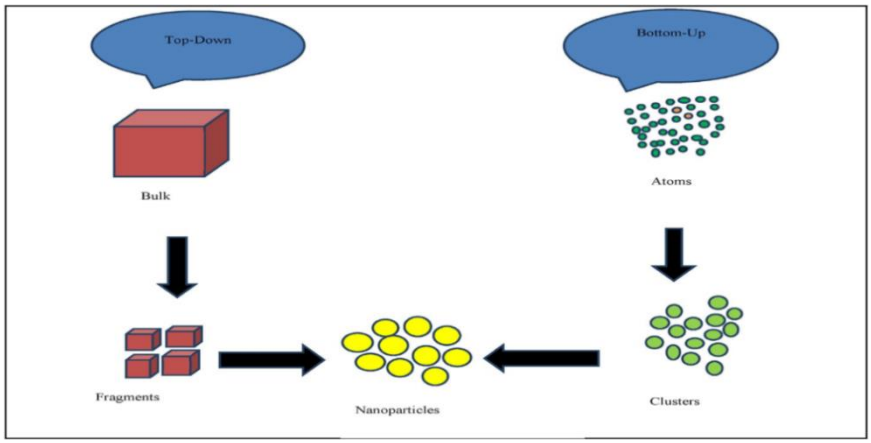

Figure I.2: Methods used in the manufacture of zinc oxide nanoparticles from the bottom up and top down [31].

I.3.2.1. Biological Method:

Some of the green routes for NP synthesis included the utilization of microorganisms, enzymes, plants, and plant extracts as potential eco-friendly alternatives to chemical or physical methods. Hosts were also used in physical and biological systems' synthesis of NPs like bacteria, fungus, and yeast. [33]

I.3.2.2. Physical Method:

For this, small particles are associated under the action of physical forces to stabilized well-defined NPs: physical fragmentation, colloidal dispersion, amorphous crystallization, and vapor condensation [34].

I.3.2.3. Chemical Method:

Methods involved in preparing ZnO-NPs are sol-gel, chemical reduction, precipitation, microemulsion, hydrothermal methods, and others. There are three basic modes in chemical procedures for the preparation of ZnO nanocomposites: solid-phase, liquid-phase, and vapor-phase (often called "wet chemical processes"). [35] The main features of these methods are environmental benignity, low energy input, low-cost, and easy to handle chemicals with simple equipment. [36] Chemical methods incorporate chemical reactions for the synthesis of nanoparticles.

a) Sol-Gel:

The sol-gel process initiates by the formation of a colloidal solution that will transform into a gel and finally into the solid material. Afterwards, the gel is heated and otherwise treated such as by evaporating off solvents, so as to arrive at the finished good. [37]

b) Hydrothermal:

A simple approach to obtaining highly crystalline metal oxide NPs is fast, cheap production through the use of an autoclave at relatively high pressure and temperature in hydrothermal mixtures. High temperatures and pressures dissolve intractable or insoluble materials.

These processes are hydrothermal or solvothermal techniques that can either use water as a solvent or organic solvents like ethanol or polyols.

c) Micro-emulsion:

For the production of ZnO-NPs, is highly used Zn sources, surfactants, and other reagents in concert with a reversed micro-emulsion system [39].

d) Precipitation

The procedure is very simple; the reactions of zinc salts, such as $Zn(NO_3)_2$, $Zn(CH_3COO)_2 \cdot 2H_2O$, and $ZnSO_4 \cdot 7H_2O$ with LiOH, NH_4OH, and NaOH under basic solutions can be covered in the synthesis procedure. It includes the reaction of zinc with hydroxide ions that precipitates out. Stable colloid suspensions of zinc oxide nanoparticles are typically prepared in an alcohol solution because in aqueous solutions, [40] $Zn(OH)_2$ is formed. Changing several parameters of the precipitation process, such as solution concentration, pH, nature of washing medium, or calcination temperature, will help obtain different morphological zinc oxide NPs. [41]

I.4. Characterization of ZnO-NPs:

A. infrared spectroscopy:

If infrared (FTIR) radiation hits a compound, part of its energy is used. The radiation that passes through the sample is measured. Since it uses monochromatic light, it can measure only one spectrum. [42]

B. UV–visible spectrophotometry

This is a technique for comparing an analytical sample against a reference or blank sample to realize the many discrete wavelengths of UV or visible light either absorbed by or transmitted through the sample. The sample composition dictates this property, hence opening ways to information about what the sample may contain and what its concentration might be as the wavelength of ZnO-NPs can be estimated by monitoring the quantity of light absorbed or scattered by a given sample. [43]

C. X-ray diffraction

X-ray diffraction is a speedy analytical technique used to determine material type, phase, and crystal characteristics. It does this by interpreting X-rays that return to the

surface of specimen. Notably, the purity of the generated CNOs can be assessed. For evaluating the crystallinity of ZnO-NPs, the X-ray diffraction technique can be used. [44]

D. Dynamic light scattering (DLS)

The most common technique is dynamic light scattering, where the hydrodynamic particle size and distribution are measured. Although coherent light sources were only invented in the 1970s, DLS has been applied in measurements to quantify macromolecules and low volumes of small particles in diluted solution. [45]

E. Zeta potential:

Measurement of the surface charge on small particles in liquid is extremely troublesome, but it is approximated using zeta potential. That has an influence on the pharmacokinetic behavior of any nanomaterial and can be ascertained by applying an electric field to a dispersion, where particles will move toward oppositely charged electrodes in proportion to the zeta potential's magnitude [45].

I.5. Antimicrobial activity and Mechanisms of ZnO particles:

The possible mechanisms for the antimicrobial action of ZnO may be based on definite interaction that is mediated through their unique physicochemical properties. ZnO-NPs combat a number of microorganisms, including fungi and bacteria.

I.5.1. Antibacterial activity:

The mechanisms involved in the antibacterial activity of ZnO-NPs are due to major processes; among these, ROS production may be stated as major, which includes superoxide anions and hydroxyl radicals, such as these highly reactive ROS, causes DNA, protein, and bacterial cell wall/membrane damage leading finally to cell death. Additionally, under UV light, ZnO-NPs function as photocatalysts in producing some of the reactive species that may further play a role in the disintegration of bacterial cell walls and membranes.

Photocatalytic activity further reinforces the overall antibacterial effect of ZnO-NPs. Finally, extensive interactions also happen between ZnO-NPs and bacterial cells.

The high surface area-to-volume ratio of ZnO-NPs enables them to adhere strongly to bacterial cell walls. The adhering material may disrupt both the cellular structure and function. In addition, ZnO-NPs cause the release of Zn2+ ions into the environment.

These ions then further bind with cell proteins, nucleic acids, and other important constituents in order to disrupt bacterial metabolism. This additional mode of action would ensure bacterial inhibition and ultimate bactericidal activity by ion release. [46,47].

Electrostatic interactions between ZnO NPs and cellwalls resulting in destroying bacterial cell integrity [48].

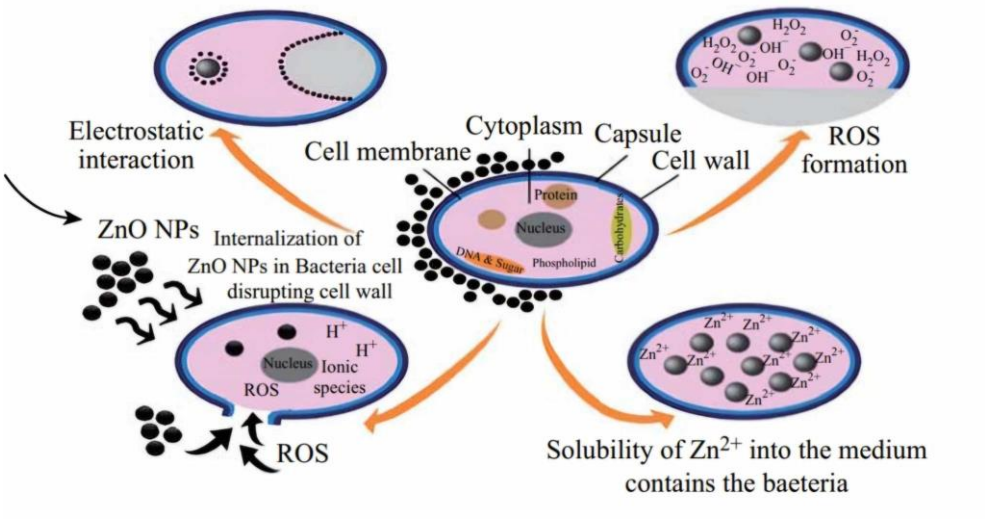

Figure I.3: different possible mechanisms of ZnO-NPs antibacterial activity, including: ROS formation, Zn^{2+} release, internalization of ZnO-NPs into bacteria, and electrostatic interactions [48].

The antibacterial potential of ZnO-NPs has been already reported against wide range of bacterial strains. Both Gram-positive (S. aureus, S. epidermidis, Streptococcus pyogenes, Bacillus subtilis) and Gram negative (E. coli) and microorganisms have been successfully attenuated using these nanoparticles. Increased ZnO NPs or Zn^{2+} concentrations generally showed stronger antibacterial activity [49].

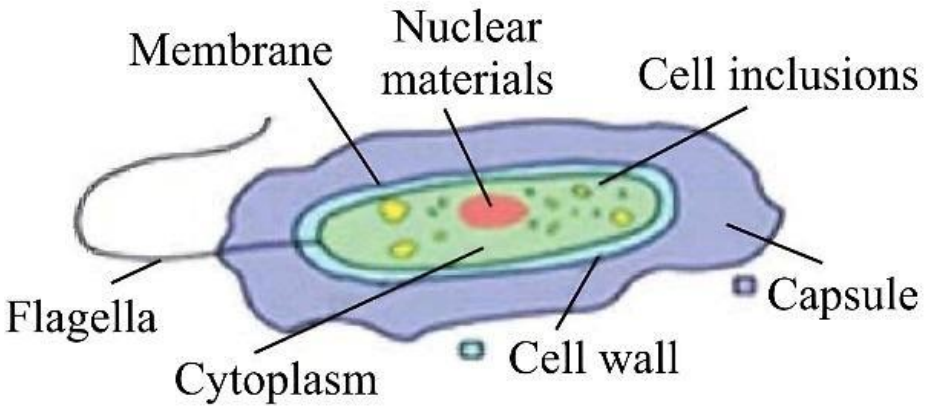

Figure I.4: Bacterial cell structures [49].

I.5.2. Antifungal activity:

The antifungal activity of ZnO NPs was confirmed against several pathogenic yeasts and fungi, and in fact such NPs are considered as a potent antifungal supplement for the food sector. It's been shown that fungi are in direct contact with ZnO-NPs through cell walls/membranes.

Their high surface to volume ratio makes these nanoparticles able to strongly adhere on the fungal structures, which can disrupt cell wall and membrane permeability.

Disruption would, therefore compromise the overall structural integrity of the fungi, making them more susceptible to damage or arrest. In addition, the release of its Zn^{2+} ions can even further boost their antifungal powers through chelation with key enzymes and metabolic pathways in fungi, thus obstructing their growth and replication [47].

I.6. Toxicity Assessments:

Despite the numerous benefits and possible nanoparticles use against bacteria, there are, however, a lot of doubts cast in this area of their toxicity toward human health risk.

While the metallic nanoparticles exhibit much more toxicity against bacteria in relation to eukaryotic cells, this should not discount their broad distribution and accumulation over time, since the same mechanisms that effectively target bacteria may just as well lead to possible collateral effects for humans. [50]

ROS production induced by the nanoparticles and stress on the body have been related to inflammatory processes in charge of the generation of a spectrum of disorders, including pulmonary diseases and liver degeneration [51].

To bring down the toxicity of ZnO nanoparticles in order for them to be applicable in medicine, for instance in drug or gene delivery purposes, different substances are often used in the surface modification. Principal among these are PEGs, well known in biology and medicine for very good biocompatibility and biodegradation [52]. It has been reported that this kind of NP modification was very effective in inhibiting oxide nanoparticles' cytotoxicity [53].

CHAPTER Ⅱ:

TRANSDERMAL DIFFUSION AND ANTIBACTERIAL ACTIVITY OF ZnO NPs INCORPORATED INTO HYDROGEL

CHAPTER Ⅱ: TRANSDERMAL DIFFUSION AND ANTIBACTERIAL ACTIVITY OF ZnO NPs INCORPORATED INTO HYDROGEL

The skin acts as a protective barrier, and it also regulates body functions related to temperature and synthesizing vitamin [54]. Common problems of the skin include wounds; their four-step healing involves hemostasis, inflammation, proliferation, and remodelling. Wound dressings, particularly those based on carbomers, with their high water content, lack of adhesiveness, and cooling effect, are perfect for the treatment of wounds. The carbomer-based hydrogels are common drug delivery systems transdermally used for the fact they are biocompatible and ensure proper release of the drug [55].

II.1. Transdermal drug delivery system

The transdermal drug delivery system is a term usually defined as topically administered drugs that are self-contained in a discrete dosage form of a patch, which, on application to the skin, delivers the drug through the skin portal to systemic circulation at a predetermined controlled rate over an extended period of time [56].

II.1.1 skin barrier:

To achieve effective transdermal delivery, the active molecules need to penetrate through the epidermis into the blood circulation system before reaching the hypodermis. Stratum corneum is the outermost layer of the epidermis and is regarded as the main barrier to drug penetration. Approximately 10 μm thick, it is composed of 15 to 20 layers deads corneocytes and the lipids are embedded in a rich matrix, yielding a 'brick-and-mortar' kind of structure [58].

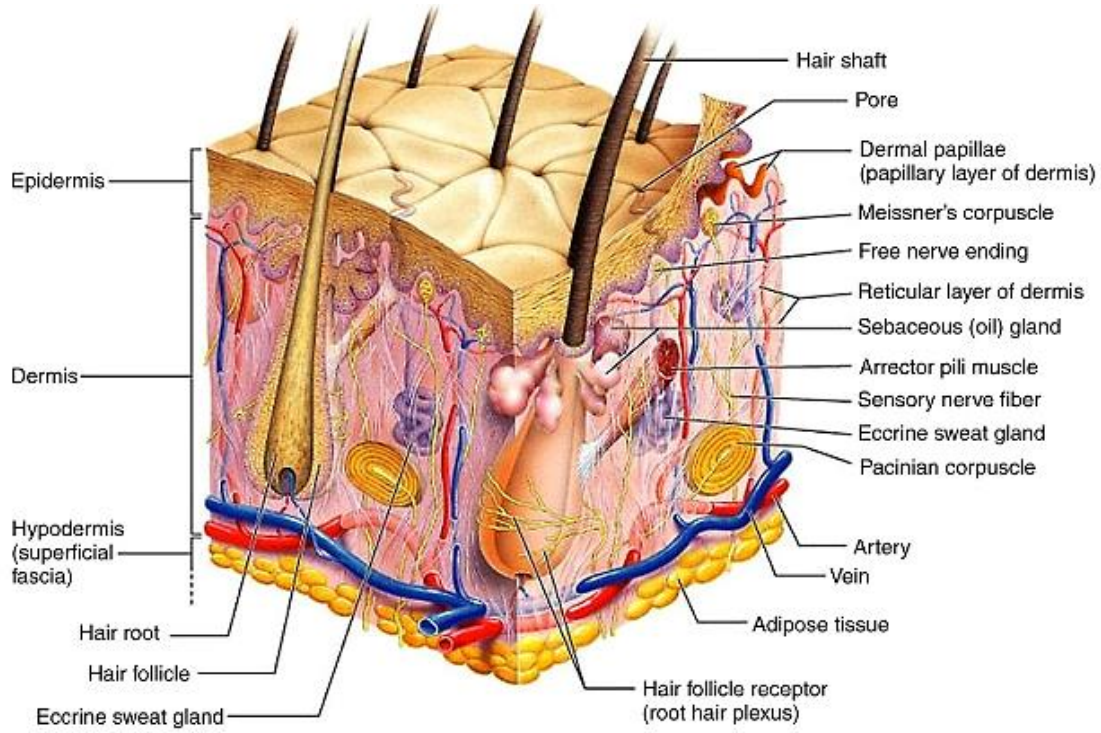

Figure II.1: Skin anatomy [57].

This lipid domain is very important for drug delivery. The composition, in the course of epidermal differentiation, switches from polar lipids to a neutral lipid mixture consisting of ceramides and some fatty acids [59].

The permeation of drugs through the skin predominantly takes place by one of three routes: transcellular, intercellular, or transappendageal (through sweat glands and hair follicles). Of the three, the most common mode of drug diffusion through the SC is said to be intercellular [60].

II.1.2. Parameters affecting the mechanism of transdermal drug delivery:

There has been increasing interest in the dermal delivery of drugs over the last ten years. The Factors that Regulate This Method of Drug Delivery:

II.1.2.1. Physicochemical Properties of the Active Compound:

a. Partition Coefficient:

Drugs have two types of solubility, water and lipid. The optimum partition coefficient (logK) for transdermal delivery is in the range from 1 to 3. The more lipophilic the drug (logK > 3), the more exogenous intracellular route becomes involved, though for drugs with low lipophilicity (logK < 1) the transcellular penetration is the major pathway.

b. Molecular Size:

The larger the molecule, the lesser the transdermal flux. Ideal transdermal delivery of a drug should have a molecular weight less than 400 nm.

c. Solubility and Melting Point:

Most organic solutes have high melting points and low solubility at standard temperature and pressure. At the same time, lipophilic drugs are expected to permeate through the skin more easily than hydrophilic drugs; they should also be water-soluble in a way.

d. Ionization:

Permeation of a drug through the skin takes place according to the pH-partition hypothesis.

e. Diffusion Coefficient:

At a constant temperature, the diffusion coefficient of any particular drug will depend mostly on the drug's properties and the interaction between the medium of diffusion.

II.1.2.2. Physicochemical Properties of the Drug Delivery System:

- Nature of active compound, pH of active compound, partition coefficient of active compound.
- Though the composition of the drug delivery system may not affect the release properties directly, it can significantly influence skin permeability.
- Most drugs do not permeate the skin efficiently for therapeutic use; hence, permeation enhancers were used to synergistically potentiate the action without altering their own properties [61].

II.1.2.3. Physiological Properties:

These include:

- Newborns and infants have a skin barrier that is hydrophobic, dry, rough, and stabilizes around the third month of life.
- Aged skin is marked by decreased moisture content, breakdown of the epidermal junction, and reduced surface area available for drug transmission to the dermis.
- Race differences (e.g., between black and white skin).
- Skin temperature [61].

II.2. Hydrogels as drug carriers:

The 3D network structure in a hydrogel with high water content results in high porosity, which can be used for encapsulating and delivering drugs in a controlled manner. The above attributes may be modulated with the cross-linking degree of the gels and the chemical moieties on the polymeric chains. [62]

Many studies have reported the potential of hydrogels in dermal and transdermal drug delivery. Indeed, one of the advantages of hydrogels, besides protecting the active ingredient, is that they provide a sustained release of the drug. [63]

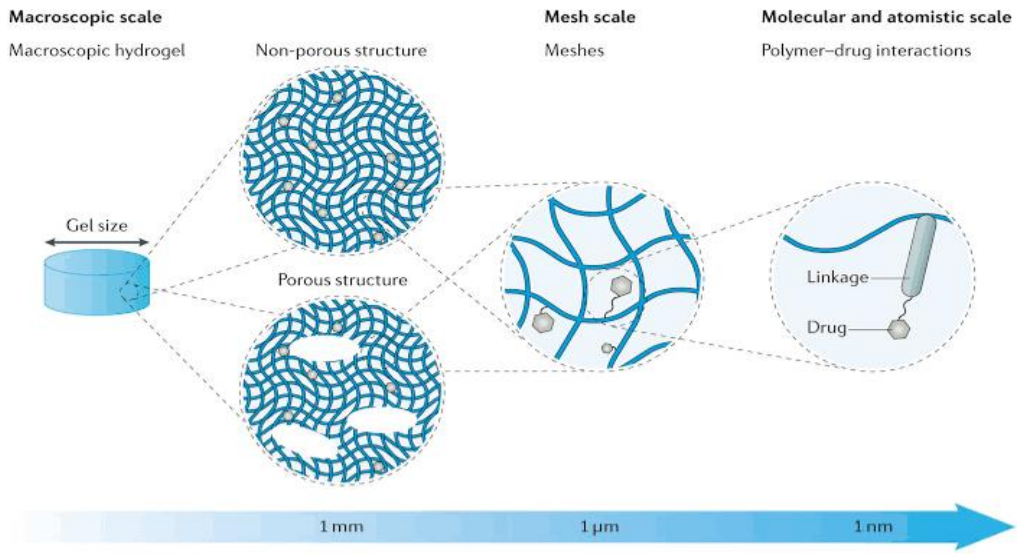

Figure II.2: Designing hydrogels for controlled drug delivery [62].

II.2.1. Key Properties of Hydrogels:

When used as biomaterials in biotechnologies, hydrogels must meet such physicochemical requirements as biocompatibility [65], mechanical strength [66], and permeability most particularly, on entrapment of drugs for controlled release applications [64,67].

Another advance in this regard is that smart hydrogels can be designed to respond to external changes of pH or temperature [68].

a. Degradability

The reason for the biomedical use of hydrogels lies in the controlled degradation of the same. In this aspect, degradable material may give space for new tissue formation or allow for the release of bioactive molecules.

That can be optimized by polymer composition, molecular weight or the application of physical, chemical, and biological methods. For instance, irradiated high molecular weight alginate breaks selected bonds to give a gel that easily degrades. Enzymatic-mediated degradation is also applied on a wide scale [65].

b. Mechanical Properties

The mechanical properties of hydrogels are dependent on their end use, such as low modulus gels for contact lenses and food applications, high modulus gels for uses in tissue engineering and biomedical implants.

Models of elasticity and viscoelasticity can describe the mechanical behaviour. The described stiffness will depend on polymer concentration, crosslinking density, type of monomer, and synthesis conditions, such as reaction time and temperature. Generally, lower mechanical resistance is obtained with higher swelling, due to the low crosslinking density. [66, 67].

c. Porosity:

Hydrogel porosity is a key parameter in the diffusion of solutes. This effective diffusion is greatly influenced by the structure, polymer composition, and solute physicochemical properties.

When the size of a solute is equal to that of the pore, one can relate the diffusion coefficients in the gel to the corresponding ones in water by means of the following model:

$$Dgel/Deau=(a,\Phi,\xi)$$

Where: **a** is the solute size, Φ the polymer volume fraction, and ξ the characteristic mesh size [69].

Typical mesh sizes range from 5 to 100 nm. Porosity can be adjusted by changing the polymer structure, crosslinking density, or external conditions such as pH, temperature, and ionic strength [64,67].

II.2.2. Physicochemical parameters to master hydrogels to topical drug carriers:

For best patient compliance and clinical efficiency, the hydrogels need to meet one of the formulation requirements.

a. Spreadability:

The major attribute is spreadability, which expressed the capability of a gel to get uniformly spread over the skin in delivering a volumetric dose of drug. Poor spreading may end up in underdosing or overdosing, causing potential side effects more especially with potent drugs [70].

b. Rheology:

It characterizes hydrogel behaviour with respect to flow and deformation under external forces, more particularly of great importance for designing formulations that spread easily and are stable [71].

II.3. Nanoparticles encapsulation and release from hydrogels:

In the selection of appropriate topical drug delivery systems using hydrogels as vehicles, the choice of active ingredient plays a major role. This having optimal characteristics, it will make NPs spontaneously penetrate through the skin. NP should possess some physical and chemical features like low molecular weight, fine balance of lipophilicity, and low melting point.

However, most active ingredients cannot penetrate through the dermal or transdermal pathway spontaneously because of these special conditions required for optimum passive diffusion through the skin. [72] Nevertheless, the above limitation can be overcome.

The design of the hydrogel systems must be based on the characteristics of the drug, so as to provide a good encapsulation and optimum release.

II.3.1. Release mechanisms:

The contribution of the release mechanism to the application of that active ingredient is very high.

a. **Diffusion-Controlled Release**

One of the key release mechanisms for drug or therapeutic entrapped in hydrogel systems is by diffusion. It is basically the movement of entrapped drugs across the hydrated polymeric network of the hydrogel. Due to their hydrophilic nature and porous structure, pore sizes of hydrogels usually lie in the range of a few nanometers to hundreds of nanometers, making them facile for diffusion out of small water-soluble molecules. Usually, it leads to burst release at the initial phase of application [73] [72].

b. **Swelling-Controlled Release**

Swelling of hydrogel matrix is another major mechanism by which drugs are released in a controlled manner. In this case, the hydrogel swells up by imbibing some fluids from the surrounding environment and enhances the mobility of entrapped molecules for their efflux, which could be induced by changing the pH, temperature, or biomolecular presence. The swelling could be either spontaneous or based on stimuli-responsive systems. The release thus goes in finer turns toward site-specific release into tissues or disease conditions showing unique micro-environments [73].

c. **Chemically-Controlled Release (Degradation/Erosion)**

A third mechanism included is chemical control, mainly through degradation or erosion of the hydrogel network. Now the polymer chains would break down by processes including hydrolysis or enzymatic activity; that is when the incorporated drug or nanoparticle starts to be released. This would depend on the type of polymer, cross-linking density, and environmental conditions [73,72].

In simple terms, with nanoparticle-hydrogel systems, release can proceed through several pathways:

- (i) First, the hydrogel matrix releases the nanoparticles; the encapsulated drug follows.
- (ii) Release of the drug from the nanoparticles within the hydrogel and its diffusion out.
- (iii) A combination of both mechanisms [74].

II.4. Nanoparticle–hydrogel system:

These nanohybrid systems of the nanoparticle with hydrogels are now being developed as a new class of biomaterials. Hence, it tries to unite the advantages presented by parent materials “hydrogels and nanoparticles” thereby fulfilling any lack in delivering drugs, engineering tissues, or applications related to biomedicine wherein either nanoparticles or hydrogels individually are relevant. [75]

II.4.1. Advantages of NPs incorporated hydrogels in delivery of the antimicrobial agents:

Hybrid systems consisting of nanoparticles together with hydrogels exhibit several unique advantages related to the case of antimicrobial delivery and have immeasurable potential toward varied biomedical applications, such as tissue engineering, drug delivery, immune modulation, reduction in antibacterial resistance, detoxification, and wound healing.

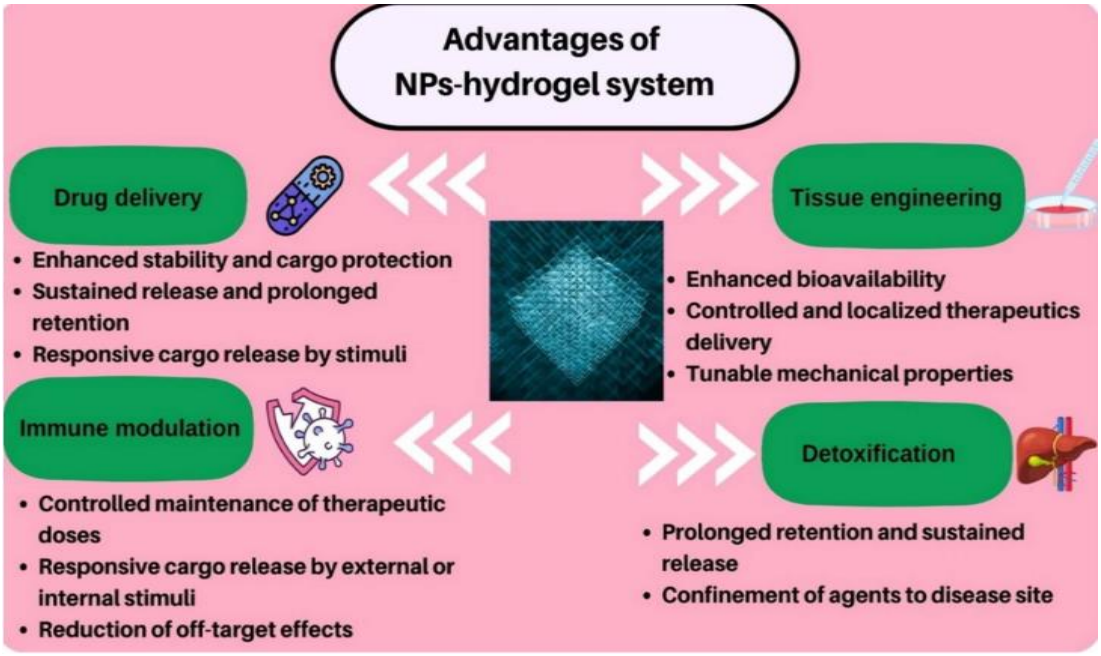

Figure II.3: Applications and advantages of nanoparticles (NPs)–hydrogel systems [76].

II.4.2. Hydrogels incorporated with zinc oxide nanoparticles:

A diverse range of nanocomposite hydrogels has been developed with the incorporation of varying types of nanoparticles in the hydrogel network. From the literature, one may deduce five principal methods of forming nanocomposite hydrogels: (1) through in situ formation of the hydrogel in the suspension of the nanoparticle; (2) blending of nanoparticles within preformed hydrogel; (3) in situ reactive nanoparticle formation within preformed hydrogel; (4) crosslinking of the hydrogel with nanoparticles; and (5) in the formulation of hydrogels using nanoparticles, cross-linking agents, and polymers. [77].

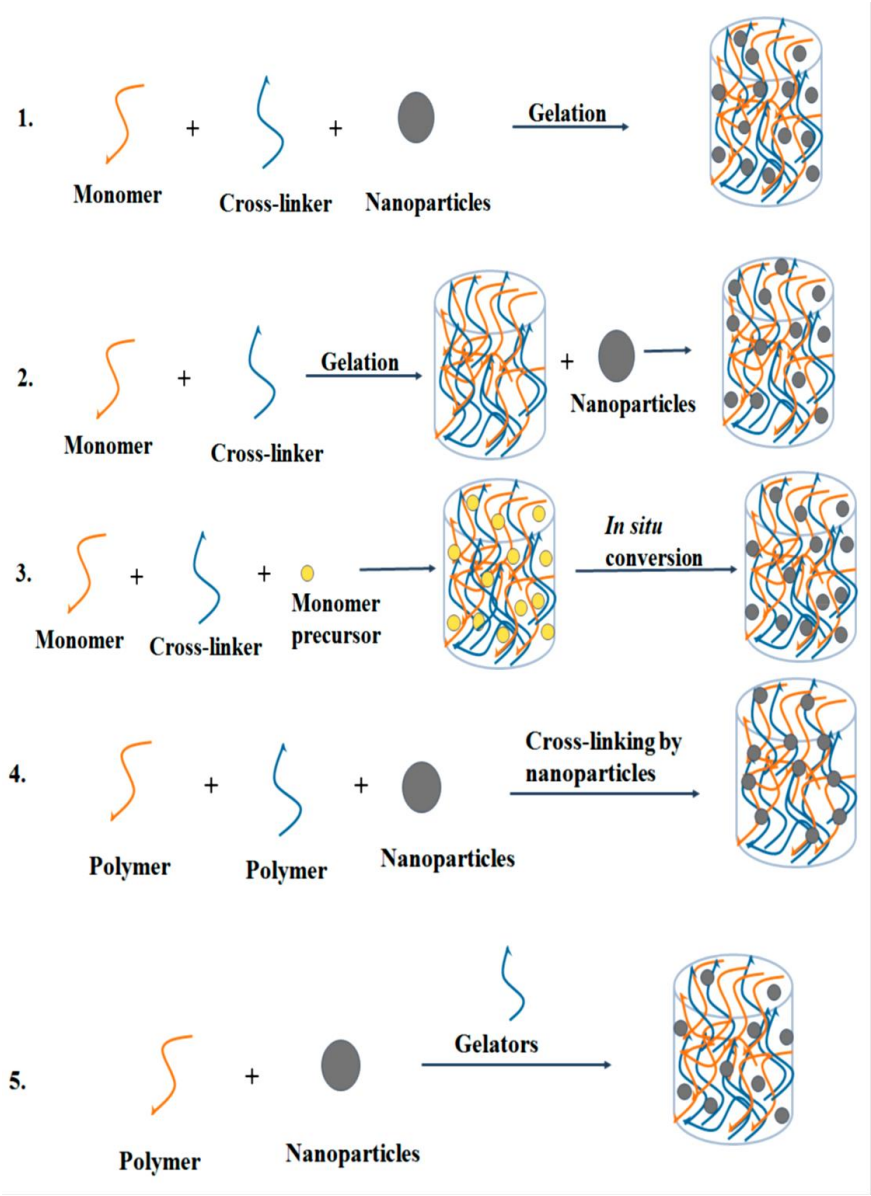

Figure II.4: the five main approaches of the incorporation of NPs in hydrogel [77].

CHAPTER III

MATERIALS AND METHODS

CHAPTER III: MATERIALS AND METHODS

III. 1 Introduction:

The objective of this work is to formulate zinc oxide (ZnO) nanoparticles with antimicrobial properties for potential application in the pharmaceutical field. and Incorporation of ZnO nanoparticles into the hydrogel matrix. In this chapter we will present the different product used and the methods of fabrication and characterisation.

III.2. Reagents and Materials

All the products and equipment used were available in the product storage and laboratories of the Process Engineering Department, where the experimental work was carried out.

III.2.1 Reagents:

❖ ***Reagents Used for ZnO Nanoparticle Synthesis:***

Zinc Nitrate Hexahydrate ($Zn(NO_3)_2 \cdot 6H_2O$):

Used as the zinc precursor in the chemical precipitation method.

Physicochemical Characteristics:

- Molecular Weight: 297.49 g/mol
- Appearance: White crystalline solid
- Solubility: Highly soluble in water Melting Point: ~36.4°C

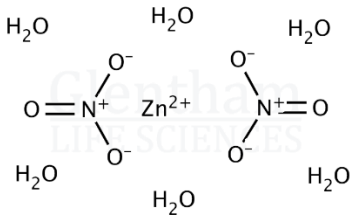

Figure III.1: chemical structure of Zinc Nitrate Hexahydrate.

Polyvinylpyrrolidone (PVP):

Used as a stabilizing and capping agent in ZnO nanoparticle synthesis to prevent agglomeration.

Physicochemical Characteristics:

- Molecular Formula: $(C_6H_9NO)n$
- Appearance: White powder
- Solubility: Soluble in water and ethanol
- Function: Stabilizer and dispersant

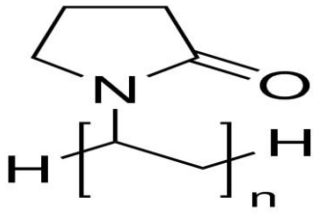

Figure III.2: chemical structure of PVP.

Ascorbic acid (AA)

It is a natural organic compound with antioxidant properties, widely used as a reducing agent in nanoparticle synthesis. In the context of ZnO nanoparticle synthesis, it promotes the reduction of zinc ions to form stable oxide particles while minimizing aggregation.

Physicochemical Characteristics

- Chemical formula: $C_6H_8O_6$
- Molecular weight: 176.12 g/mol
- Appearance: White to slightly yellow crystalline powder
- Solubility: Soluble in water (330 g/L at 20 °C)
- pH (1% solution): 2.2 – 2.5

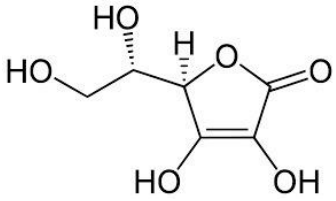

Figure III.3: Chemical structure of Ascorbic acid.

Ethanol:

It is a clear, colourless, volatile liquid commonly used as a solvent and antiseptic. In ZnO nanoparticle synthesis, it serves as a washing agent or helps to adjust viscosity and promote solubilisation.

Physicochemical Characteristics:

- Chemical formula: C_2H_6O
- Molecular weight: 46.07 g/mol
- Appearance: Clear, colourless liquid
- Boiling point: 78.37 °C
- Solubility: Miscible with water
- Function: Washing agent for ZnO NPs

Sodium Hydroxide (NaOH):

Used to precipitate Zn^{2+} ions by adjusting pH.

Physicochemical Characteristics:

- Molecular Weight: 40.00 g/mol
- Appearance: White solid (pellets)
- Solubility: Soluble in water (exothermic)
- pH (0.1M): ~13

❖ ***Excipients Used in Hydrogel Formulation:***

Carbopol 940:

Carbopol is a high molecular weight, cross-linked polyacrylic acid polymer. It is widely used as a gelling and thickening agent in pharmaceutical and cosmetic formulations. It helps in forming transparent hydrogels with high viscosity and good bioadhesive properties.

Physicochemical Characteristics:

- Chemical Description: Cross-linked polyacrylic acid polymer
- Molecular Weight: Approx. 72,06 g/mol
- Appearance: White powder
- pH (0.5% solution at 25°C): 2.7 – 3.3
- Viscosity (0.5% at 25°C): 400,000 – 600,000 mPas
- Solubility: Dispersible in water, neutralized to form a gel

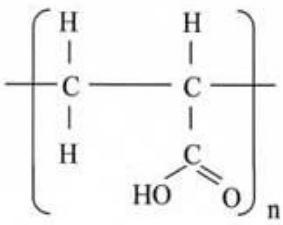

Figure III.4: chemical structure of Carbopol 940

Glycerol:

Glycerol is used as a humectant and plasticizer. It improves the consistency of the gel and prevents drying out.

Physicochemical Characteristics:

- Chemical Formula: $C_3H_8O_3$
- Molecular Weight: 92.09 g/mol
- Appearance: Clear, colorless, viscous liquid
- Boiling Point: 290°C
- Solubility: Miscible with water

Triethanolamine (TEA):

TEA is used as a neutralizing agent for Carbopol. It raises the pH and induces gelation.

Physicochemical Characteristics:

- Chemical Formula: $C_6H_{15}NO_3$
- Molecular Weight: 149.19 g/mol
- Appearance: Colorless, viscous liquid
- pH (1% solution): ~10.5

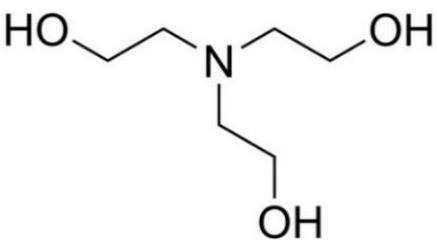

Figure III.5: chemical structure of TEA.

III.2.2. Materials:

This part includes all the equipment used to synthesize the ZnO NPs, formulate the hydrogels and then their characterization.

The table below presents all the equipment used to synthesize the ZnO nanoparticles and formulate the hydrogels.

Table III.1: Equipment used for the synthesis of ZnO NPs hydrogel formulation.

Designation	Brand	Description
Analytical Balance	KERN EG	Used for accurate weighing of chemicals and samples.
Heating magnetic stirrer	AREC VELP scientifica	Used for uniform mixing and dissolution of substances.
Homogenizer	WiseTis homogenizer (hg-15d)	Employed to obtain a uniform and smooth texture of gels or suspensions.
Sonicator	BRANSON Digital Sonifier	Facilitates nanoparticle dispersion by ultrasonic waves.
pH meter	HANNA instruments HI 2210 pH meter	A digital instrument used to measure the hydrogen ion concentration (pH) of aqueous solutions.
Mortar Grinder	mLm KM1	Used for fine grinding and homogenization of powders.

The table below presents all the equipment used in the characterization of the ZnO nanoparticles and hydrogels.

Table III.2: Equipment used for the characterization of ZnO NPs and hydrogel formulation.

Designation	Brand	Description
UV-Visible Spectrophotometer	Shimadzu UV-1900i	Analyzes absorbance and concentration of substances.
X-ray Diffraction (XRD)	Rigaku XRD diffractometer	Determines the crystalline structure of nanoparticles.
Dynamic Light Scattering and Zeta Potential Analyzer	Horiba scientifica nanoparticle analyzer SZ-100	Measures particle size distribution in nanomaterials. Determines surface charge and stability of nanoparticles.
Rheometer	Anton Paar modular compact rheometer MCR 302	A device used to measure the flow and deformation behaviour (viscosity and elasticity) of semi-solid formulations.
Fourier Transform Infrared Spectrophotometer (FT-IR)	Paragon 1000 FTIR Perkin Elmer	A spectroscopic instrument that detects functional groups and chemical bonds in a sample.

III.3. Experimental Procedures:

In this chapter, we describe the experimental procedures used for the synthesis of zinc oxide nanoparticles, the formulation of hydrogels, and the incorporation of the nanoparticles into the hydrogel matrix.

III.3.1. Synthesis of ZnO Nanoparticles:

Under a heating magnetic stirring at 60 °C, a polyvinylpyrrolidone (PVP) solution was added to a zinc nitrate hexahydrate [$Zn(NO_3)_2 \cdot 6H_2O$] solution. Subsequently, 0.2 M sodium hydroxide (NaOH) was added dropwise to the mixture until a pH of 7 was reached, resulting in the formation of a white precipitate of zinc hydroxide [$Zn(OH)_2$], which then thermally decomposes into ZnO:

$$Zn(NO3)2\,.6H2O\ (aq)\ +\ 2NaOH\ (aq) \rightarrow Zn(OH)_2\ (s) + 2NaNO_3\ (aq) + 6H_2O\ (l)$$

$$Zn(OH)_2 \rightarrow ZnO\ (s) + H_2O\ (g)$$

A fixed amount of ascorbic acid was added to the mixture as a mild reducing agent to enhance particle dispersion and minimize oxidation. After 20 minutes of continued reaction, the product was filtered, washed with distilled water and ethanol, dried in an oven at 100 °C for 6 hours, and ground to obtain a fine ZnO powder.

Figure III.6: steps for the preparation of ZnO nanoparticles.

III.3.1.1. characterization of ZnO Nanoparticles:

A preliminary organoleptic evaluation was carried out by visually inspecting the synthesized ZnO nanoparticles. Subsequently, the ZnO nanoparticles were characterized using various analytical techniques, including:

A. FTIR:

A small quantity of ZnO powder was directly placed on the ATR crystal without prior preparation. The spectrum was recorded over the range of 4000–400 cm^{-1} and expressed in transmittance (%T) to identify the functional groups present on the surface of the nanoparticles.

B. UV-Vis:

A suspension was prepared by dispersing 5 mg of ZnO powder in 50 mL of distilled water and sonicated for 15 to 30 minutes to ensure proper dispersion. An aliquot of this suspension was placed in a cuvette and analyzed using a UV-vis spectrophotometer. The absorbance was recorded over the wavelength range of 350 to 380 nm, corresponding to the characteristic absorption band of ZnO nanoparticles [79].

C. DLS:

For this analysis, 5 mg of ZnO powder was dispersed in 50 mL of distilled water, and the suspension was sonicated for 30 minutes at room temperature to ensure proper dispersion. After sonication, the sample was successively filtered using 0.45 µm and 0.22 µm syringe filters before being analysed. The refractive index of ZnO was considered as 2.0 during the measurement [78].

D. Zeta Potential:

The zeta potential analysis was performed using the same instrument, therefore the same sample prepared for the DLS analysis.

E. XRD:

A small amount of ZnO powder was placed on the sample holder without any prior treatment. The analysis was performed over an appropriate 2θ range, allowing the identification of characteristic peaks related to the crystalline structure of the nanoparticles.

III.3.2. Formulation for hydrogels:

Carbopol 940 was dispersed in distilled water under continuous magnetic stirring until complete polymer dispersion was achieved. Triethanolamine (TEA) was then gradually added to neutralize the dispersion and induce gelation. Finally, glycerol was incorporated as a humectant, and the final volume was adjusted with distilled water. Different Carbopol concentrations were tested to optimize viscosity and stability.

The table below presents the formulations of five hydrogels containing different concentrations of Carbopol, ranging from 0.2% to 0.6%.

Table III.3: hydrogels formulations with different carbopol concentration

S. No	Ingredients	F1	F2	F3	F4	F5
1.	Carbopol 940	0.2%	0.3%	0.4%	0.5%	0.6%
2	Triethanolamine	1%	1%	1%	1%	1%
3	Glycerol	1%	1%	1%	1%	1%
4	Distilled water	q.s. to 100ml	q.s. to 100ml	q.s. to 100ml	q.s. to 100ml	q.s. to 100ml

III.3.2.1. characterization of the hydrogel

The characterization of the hydrogels included organoleptic analysis, pH measurement, the rheological study, spreadability test, swelling test and FTIR.

A. Rheological study:

Following the formulation of the hydrogels, it is essential to evaluate their rheological behavior. This analysis was performed using a modular compact rheometer (Physica Rheolab MCR302, Anton Paar).

The measurement system employed was a cone-plate configuration. Rheological properties and parameters depend on the applied stress and the duration of its application. The tests were conducted at 20°C after allowing the gels to rest for at least 24 hours to ensure equilibrium.

Figure III.7: Rheological measurements were conducted using a cone-plate system.

Two types of tests were carried out: a viscoelasticity test to define the linear viscoelastic region and determine the viscoelastic components, and a flow test to assess the flow behaviour of the gels.

1. The viscoelasticity test was performed while recording the two viscoelastic moduli, namely the storage modulus (G') and the loss modulus (G'').

Two types of measurements were performed:

- *Strain Sweep (Amplitude Sweep):*

This test was carried out at a constant frequency by gradually increasing the strain by varying γ from 10^{-3} to 10^{3}%. It helps to identify the Linear Viscoelastic Region (LVR), within which the material structure remains undisturbed and the moduli (G' and G'') remain constant.

- *Frequency Sweep:*

In this test, the frequency was decreased from 100 to 10^{-2}% while keeping the strain constant (within the LVR). It provides information on the time-dependent viscoelastic behaviour of the material. A higher G' compared to G" across the frequency range indicates a predominantly elastic character.

2. The flow test involved varying the shear rate from 10^{-3} to 10^{3} s^{-1} and measuring the apparent viscosity of the samples.

B. Spreadability Test:

The test was performed using a modified parallel plate method. A sample of hydrogel was placed within a 1 cm diameter circle marked on a glass plate positioned over graph paper with concentric circles. A second glass plate was placed on top, followed by weights of 136 g, 185 g and 315 g for 30 seconds each. The increase in diameter was recorded, and spreadability was calculated using the following equation:

$$S = (\pi \times d^2) / 4$$

Where S is the spread area (cm^2) and d is the average diameter (cm).

C. Swelling Test:

Bulk hydrogel samples were prepared and dried in a hot air oven at 100 °C for 1 h. The sample was then immersed in distilled water at room temperature to allow rehydration. It weight was recorded to monitor water uptake. The swelling ratio (TG) was calculated using the equation:

$$TG = (mt - m0) / m0$$

Where TG is the swelling rate (%), m0 is the dry weight (g), and mt is the rehydrated weight (g).

III.3.3. incorporation of ZnO NPs into the hydrogel

The incorporation of ZnO nanoparticles into the hydrogel was carried out using the in situ method, where the hydrogel was formed in the presence of the nanoparticle suspension. After sonication, the ZnO nanoparticle solution was added to the previously prepared placebo gel under continuous stirring.

The formulation was then neutralized using triethanolamine (TEA) to achieve gelation.

III.3.3.1. characterization of the ZnO NPs hydrogel

During the ZnO NP/hydrogel incorporation step, characterization was carried out through pH measurement, IR analysis, rheological study, transdermal diffusion testing, antifungal and antibacterial activity evaluation.

A. transdermal diffusion testing:

In Vitro Diffusion Study The setup consisted of a Franz diffusion cell. Approximately 5mg of hydrogel loaded with ZnO nanoparticles was evenly applied onto a cellulose acetate membrane. The receptor compartment was filled with phosphate buffer solution (pH 7.4).

The cell was maintained in a water bath at 40 °C to simulate a skin temperature of 37 °C. At regular time intervals, samples were withdrawn from the receptor solution to study the diffusion of ZnO nanoparticles.

Figure III.8 : Franz Diffusion Cell Setup

Analyses were performed using a UV-Visible spectrophotometer at 364 nm. Withdrawn volumes were immediately replaced with equal amounts of fresh buffer.

The kinetic diffusion parameters were determined, including the diffusion coefficient (D), permeability coefficient (Kp), and lag time (tr), based on the experimental results obtained.

Diffusion Coefficient (D):

The diffusion coefficient (D) represents the mobility of a product through the film layer. It is calculated using the following equation:

$$D = \frac{(Q^2)}{(\pi \times 4 \times {C_0}^2 \times t)}$$

Where D is the diffusion coefficient [$cm^2.min^{-1}$], Q is the amount of drug released per unit area [$mg.cm^{-2}$], C_0 is the initial concentration of the active ingredient in the hydrogel [$mg.cm^{-3}$], and t is the time elapsed from the start of the release experiment [min].

Permeability Coefficient (Kp)

The permeability coefficient (Kp) represents the rate of permeation. It is used to assess the outcome of an absorption experiment. Its value is influenced by formulation parameters and membrane characteristics:

$$Kp = \frac{Js}{C_0}$$

Where Kp is the permeability coefficient [$cm.min^{-1}$], C_0 is the initial concentration of the active ingredient in the studied formulation [$mg.cm^{-2}$], and Js is the flux at equilibrium [$mg.\ cm^{-2}.min^{-1}$].

Flux at Equilibrium (Js):

It is determined from the slope of the linear portion of the absorption kinetics curve (Q = f(t)). This represents the steady-state flux and is typically obtained from ex-vivo experiments, where the concentration in the donor compartment is maintained constant (infinite dose conditions), and the receptor solution ensures that the concentration of the substance is either zero or very low.

Lag Time (tr)

The linear portion of the absorption kinetics curve can be extrapolated to the time axis to determine the lag time. According to Fick's second law of diffusion, this can be mathematically expressed as:

$$tr = \frac{h^2}{6D}$$

The modelling of transdermal diffusion kinetics was carried out using four different models: zero-order, first-order, Higuchi, and Korsmeyer–Peppas, as shown in the table below.

Table III.3: Modelling of transdermal diffusion kinetics.

Mathematical models	Equation	Graph	Reference
Zero-order	$\frac{Qt}{Q\infty} = K0\,.\,t$	Q = f(t)	(Aucoin, 2013)
First-order	$\frac{Qt}{Q\infty} = e - K1.t$	Ln Q = f(t)	(Aucoin, 2013)
Higuchi	$\frac{Qt}{Q\infty} = Kh.\mathrm{T}1/2$	Q = f ($t^{1/2}$)	(Aucoin, 2013)
Korsmeyer peppas	$\frac{Qt}{Q\infty} = K.tn$	Log Q = f (log t)	(Aucoin, 2013)

Where Qt/Q∞ represent the fraction of ZnO nanoparticles released from the hydrogel; t is the time; K_0, K_h, K_1, and K are the kinetic constants; n is the release exponent that depends on the release mechanism. [79, 80]

B. Antimicrobial activity evaluation:

B.1.Antibacterial activity evaluation:

The hydrogels were assessed for antibacterial activity by agar well diffusion method against four bacterial strains, which included Escherichia coli, Pseudomonas aeruginosa, Staphylococcus aureus, and Klebsiella pneumoniae. Zone of inhibition was measured around the well containing the test samples.

Preparation of Microbial Strains:

The tests for bacterial activity have been conducted by using four types of bacterial strains. The subculture of these strains has been done, and for inoculation with a single colony into 5 mL of sterile saline solution for the revival of 24 hours at 37°C in an incubator to have proper growth phase before inoculation.

Preparation of Media:

The media that will be used for the purpose is Mueller-Hinton agar. The medium is first liquefied by heating in a dry oven at a temperature of 150°C. Approximately 15–20 mL of this molten agar is poured aseptically into sterile Petri dishes, which have been labeled before, prior to forming the required strains. The plates were allowed to solidify at room temperature on the workbench.

Inoculation of Bacterial Strains:

Once the agar had solidified, the surface of each plate was inoculated with the respective bacterial suspension using a sterile cotton swab. The swab was first immersed in the bacterial suspension and then pressed against the inner wall of the test tube to remove excess liquid.

The inoculation was performed by streaking the swab uniformly over the entire surface of the agar plate in three directions, with a rotation of approximately 60° between each streak, to ensure homogenous coverage. Finally, the swab was passed around the edge of the agar to cover the perimeter.as it's shown in the figure below.

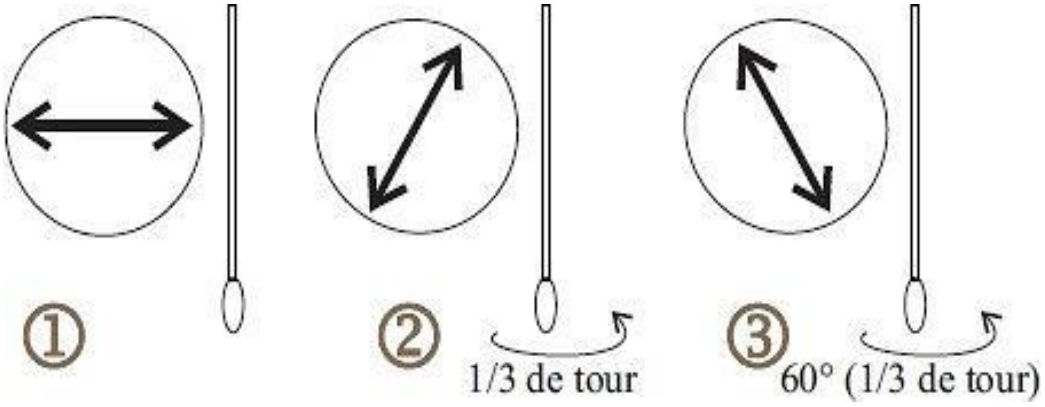

Figure III.9: 3-quadrant streak method [83].

Well Preparation and Sample Loading:

Three wells of equal diameter were aseptically punched in each inoculated agar plate using a sterile cork borer. The wells were then filled with the following formulations:

Well 1: Blank hydrogel (control)

Well 2: Hydrogel containing 2mg of ZnO nanoparticles

Well 3: Hydrogel containing 1mg of ZnO nanoparticles Care was taken to avoid any overflow or contamination between wells.

Incubation and Measurement:

The inoculated and loaded Petri dishes were incubated at 37°C for 24 hours. After incubation, the antibacterial activity was evaluated by measuring the diameter of the inhibition zones formed around each well using a ruler or calliper. The diameter of each zone was recorded in millimetres (mm), and the results were compared to assess the antibacterial efficacy of the hydrogel formulations.

B.2.Antifungal activity evaluation:

Culture Medium:

The culture medium used was Sabouraud agar supplemented with chloramphenicol (SC), supplied by Ideal Labo.

Preparation of Controls:

- Negative control: carbopol gel alone.
- Positive control: 1% econazole solution, a standard antifungal agent.

Preparation of Petri Dishes:

The melted culture medium was poured into sterile Petri dishes and allowed to solidify at room temperature.

Well Formation:

Wells were created in the agar using sterile tips, previously sterilized in an autoclave at 121°C for 15 minutes.

Fungal Inoculation:

The agar surface was inoculated with a sterile swab soaked in a fungal spore suspension, prepared from young fungal cultures.

Sample Introduction:

The different gels (blank hydrogel, hydrogel + ZnO, controls) were introduced into the wells using a sterile swab or micropipette.

Incubation:

The plates were incubated at the appropriate temperature (typically 28–30°C) for 24 to 48 hours.

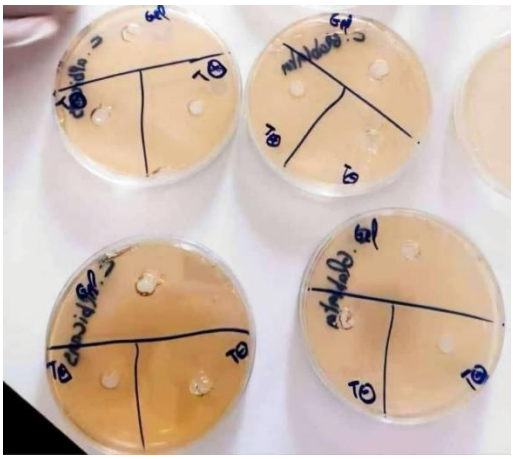

Figure III.10: Zone of Inhibition Indicating Antifungal Activity.

CHAPTER IV

RESULTS AND DISCUSSION

CHAPTER IV: RESULTS AND DISCUSSION

In this chapter, we present and discuss the results obtained from the synthesis and characterization of zinc oxide nanoparticles, the formulation and characterization of hydrogels, the incorporation of the nanoparticles into the hydrogel matrix, and the evaluation of their diffusion behaviour and antimicrobial activity.

IV.1. Characterization of Zinc Oxide Nanoparticles:

Once synthesized, the ZnO nanoparticles were characterised to ensure their quality, using various analytical techniques, as detailed below:

IV.1.1. Visual characteristics of ZnO nanoparticles:

The ZnO nanoparticles appear as a smooth, crystalline, and lightweight powder, with a colour ranging from white to yellowish-white, in accordance with the specifications described in the 11th edition of the European Pharmacopoeia. [82]

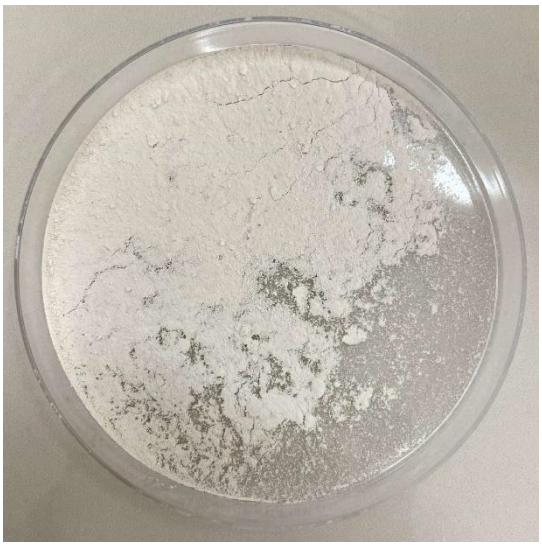

Figure IV.1: Appearance of ZnO Nanoparticles.

IV.1.2. Infrared (IR) Spectroscopy:

The IR spectra of the ZnO nanoparticles are illustrated in the following results:

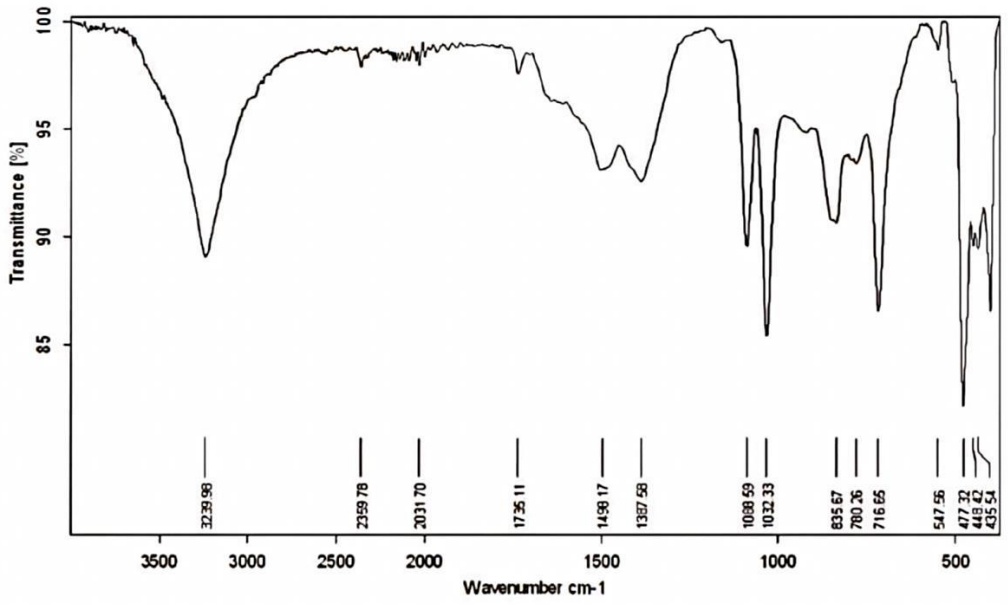

Figure IV.2: FTIR spectra of ZnO NPs

The FTIR spectrum of the synthesized ZnO nanoparticles showed characteristic absorption bands confirming the presence of key functional groups. A broad band at 3299 cm^{-1} corresponds to O–H stretching vibrations, indicating surface hydroxyl groups or adsorbed water. Peaks at 1637 cm^{-1} and 1387 cm^{-1} are attributed to H–O–H bending and C=O stretching, respectively, possibly from residual organics or atmospheric CO_2.

Notably, strong bands at 547, 477, and 432 cm^{-1} are assigned to Zn–O stretching vibrations, confirming the successful formation of ZnO nanoparticles.

IV.1.3. UV-VIS Spectroscopy:

The UV VIS results of the ZnO nanoparticles are illustrated in the following results:

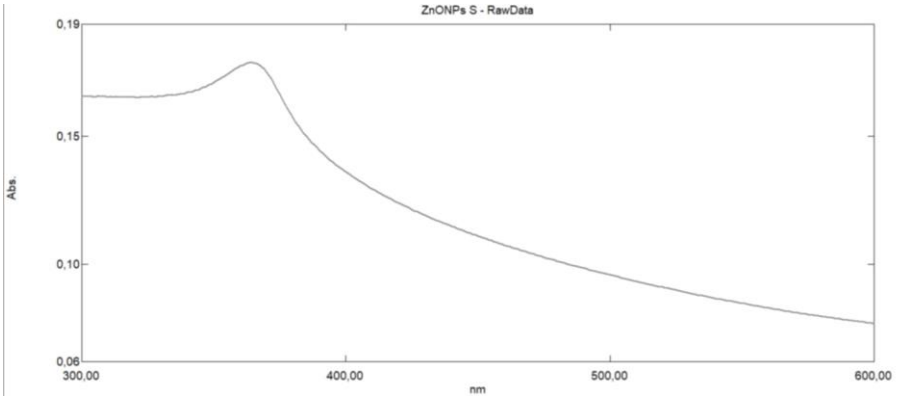

Figure IV.3: Absorption spectra of ZnO NPs.

The UV–Visible absorption spectrum of the synthesized ZnO nanoparticles displayed a sharp absorption peak at 364 nm, which is characteristic of ZnO and corresponds to its intrinsic band-gap transition.

This result is in agreement with literature values typically reported between 350 and 380 nm, confirming the nanoscale dimension and good optical quality of the particles. [79]

IV.1.4. Dynamic Light Scattering (DLS):

The dynamic light scattering analysis was conducted at a scattering angle of 90° and a temperature of 25 °C to evaluate the size distribution and dispersity of the synthesized ZnO nanoparticles. The result is presented in figure IV.4.

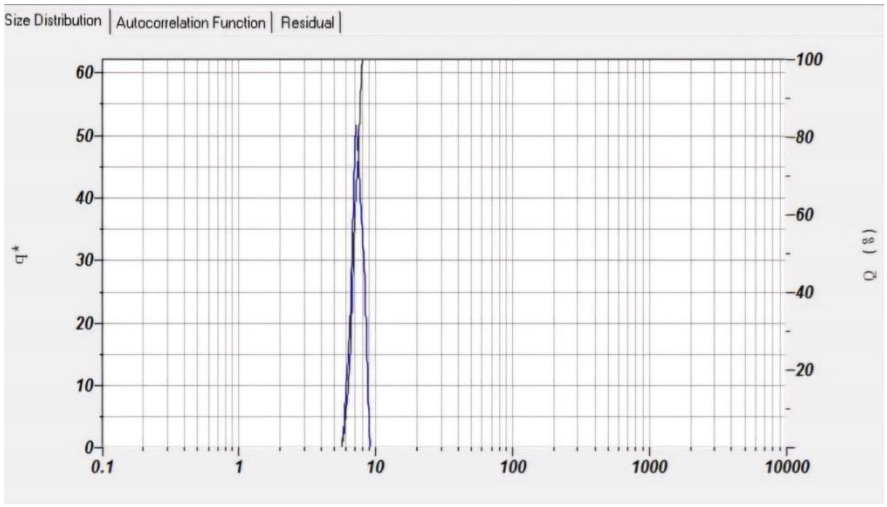

Figure IV.4: DLS size distribution of ZnO nanoparticles.

Figure IV.4 shows that the ZnO nanoparticles exhibit a Z-average (mean hydrodynamic diameter) of 6.94 nm, with a polydispersity index (PI) of 0.341.

The DLS curve displays a single sharp peak, indicating a monodisperse system composed of particles with uniform size. This monomodal distribution suggests that the ZnO suspension is homogeneous, with minimal aggregation. The measured particle size falls within the typical range reported in the literature for ZnO nanoparticles (5–20 nm), confirming the reliability of the synthesis method [78].

IV.1.5. Zeta Potential:

The figure below shows Zeta Potential Distribution Curve of Synthesized ZnO Nanoparticles:

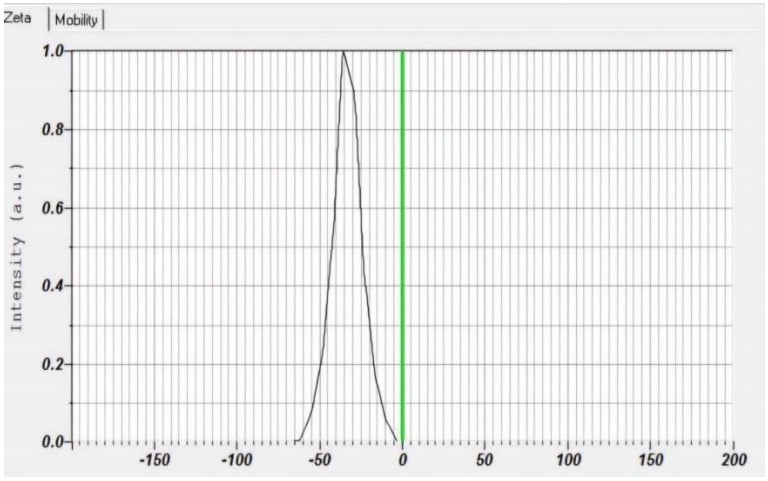

Figure IV.5: Zeta Potential Distribution Curve of Synthesized ZnO Nanoparticles.

The aqueous suspension of ZnO nanoparticles, prepared by simple dispersion in distilled water followed by sonication, exhibited a zeta potential of –33 mV, indicating an anionic surface behaviour. This negative surface charge is primarily attributed to the spontaneous adsorption of hydroxyl ions (OH^-) and the partial deprotonation of surface Zn–OH groups, occurring in a medium with a pH below the isoelectric point of ZnO.

As reported in the literature, values above ±30 mV reflect stable dispersions, confirming the efficiency of the synthesis and dispersion methods. [78]

IV.1.6. X-ray Diffraction (XRD):

The crystallographic structure of the synthesized ZnO nanoparticles was investigated using X-ray diffraction (XRD) analysis. The obtained diffraction pattern (Figure IV.6) shows multiple sharp and well-defined peaks, indicating the crystalline nature of the sample.

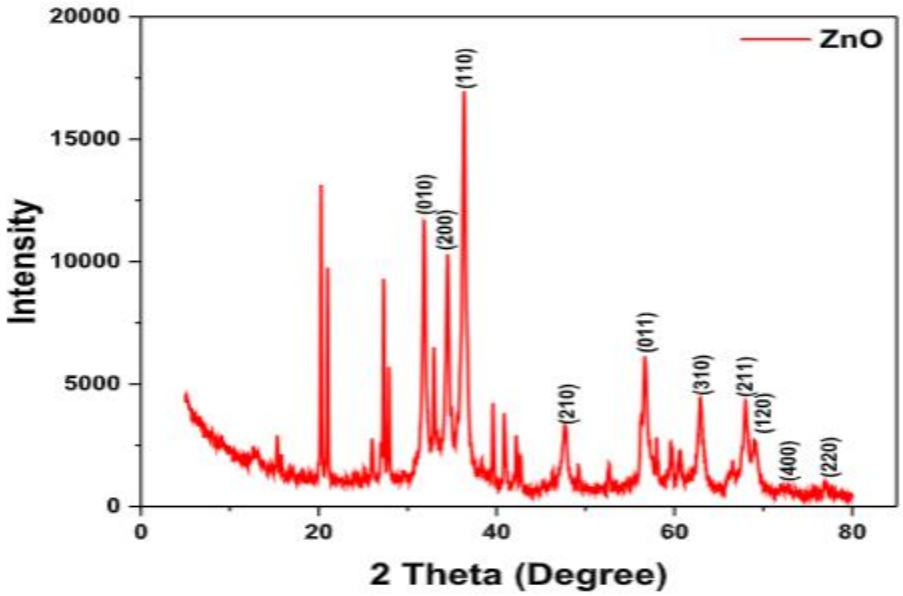

Figure IV.6: XRD patterns of the standard ZnO JCPDS card No. 36-1451 and synthesized ZnO NPs.

The peaks corresponding to the Miller indices (010), (200), (110), (210), (011), (310), (211), (120), (400), and (220) were matched with the JCPDS card no. 98-016-6243, confirming the formation of the crystalline phase structure of ZnO nanoparticles.

The presence of a few secondary peaks observed in the diffractogram may be attributed to residual impurities, likely due to experimental conditions and working constraints in the laboratory environment. Indicating that the ZnO nanopowder is not composed of pure zinc oxide.

IV.2. Characterization of the Hydrogels:

Once formulated, the hydrogels were characterized to evaluate physicochemical properties, as described below:

IV.2.1. Organoleptic parameters of the Hydrogels:

The organoleptic properties of the five hydrogels formulations were evaluated after 24 hours of preparation, and the results are summarized in the following table:

Table IV.1: Organoleptic Characteristics of the five Hydrogels.

Formulation	CP %	Appearance	Consistency	Color	Odor
F1	0.2	Homogeneous	Semi-liquid (partial gel formation)	Transparent	Odorless
F2	0.3	Homogeneous	Gel formed, viscous	Transparent	Odorless
F3	0.4	Homogeneous	Gel formed, viscous	Transparent	Odorless
F4	0.5	Homogeneous	Well-formed gel, highly viscous	Transparent	Odorless
F5	0.6	Homogeneous	Very thick and firm gel	Transparent	Odorless

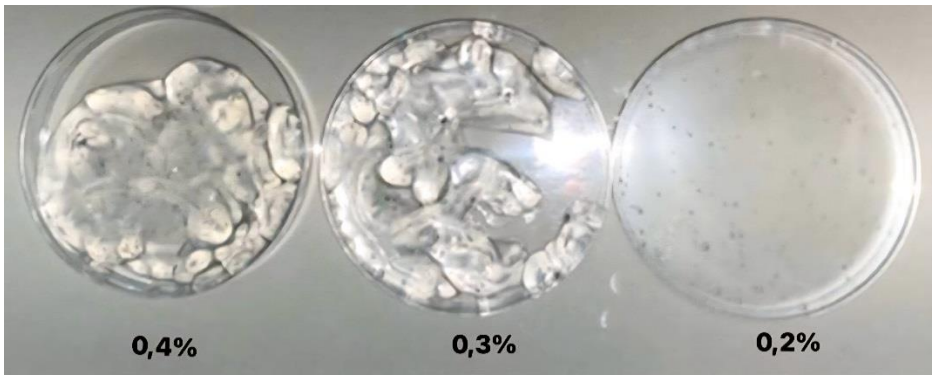

Figure IV.7: Appearance of 0.4%, 0.3% and 0.2% hydrogels respectively.

IV.2.2. pH measure of the Hydrogels:

The pH was determined using a pH meter, and the results of the five formulations are presented in the table below:

Table IV.2: pH measurement of the five Hydrogels.

Formulation	F1 (0.2%)	F2 (0.3%)	F3 (0.4%)	F4 (0.5%)	F5 (0.6%)
pH	6.82	6.38	6.23	6.11	5.91

The measured pH values of the formulated hydrogels are close to neutrality, making them suitable for topical application without causing skin irritation, as the natural skin pH ranges between 5.5 and 6.6.

IV.2.3. Rheology study:

IV.2.3.1 Viscoelasticity Test Results:

The results of this test clearly demonstrate the viscoelastic behaviour of all the prepared hydrogels, as evidenced by the presence of the two viscoelastic moduli, G' and G". G', the storage modulus, represents the elastic (solid-like) component of the fluid, while G", the loss modulus, corresponds to the viscous (liquid-like) component.

The figure below shows rheological characterization of the Hydrogel: Strain and Frequency Sweep Analyses of Storage Modulus (G') and Loss Modulus.

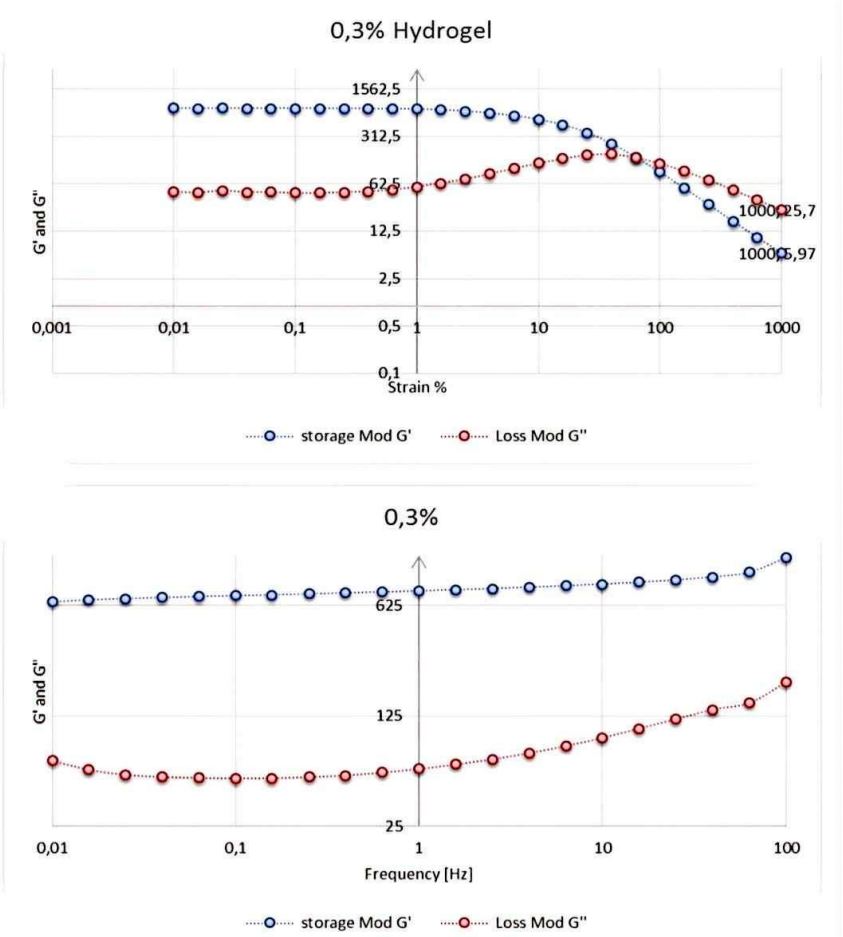

Figure IV8: Rheological Characterization of 0.3% Hydrogel: Frequency and Strain Sweep Analyses of Storage Modulus (G') and Loss Modulus (G'')

The viscoelasticity curves obtained for different Carbopol concentrations (0.2% to 0.6%) show that the storage modulus (G') is higher than the loss modulus (G'') at low strain levels, indicating a predominantly elastic behaviour, typical of a structured gel. The crossover point between G' and G'' marks the end of the linear viscoelastic region (LVR), beyond which the gel begins to lose its internal structure.

A comparative analysis reveals that:

a. Gels at 0.5% (100% strain) and 0.6% (75.9% strain) exhibit the highest resistance to deformation, indicating a stronger gel network.
b. At 0.4% (36.1% strain), the structure appears unexpectedly weaker despite the higher concentration.

c. The 0.3% gel, with a crossover point at 63.1% (same as 0.2%), shows better cohesion while using less polymer, making it the most economical and efficient formulation.

Regarding frequency sweep, all hydrogels exhibited frequency-independent behaviour, where G' remained consistently higher than G'' across the frequency range. This confirms that the gels maintain their solid-like, elastic structure over time and under dynamic stress conditions. The parallel trend of G' and G'' without crossover throughout the tested frequencies reflects good mechanical stability and structural integrity, indicating that all formulations are stable and resistant to oscillatory deformation.

The figure below shows all five hydrogels curves Strain Sweep Analyses of Storage Modulus (G').

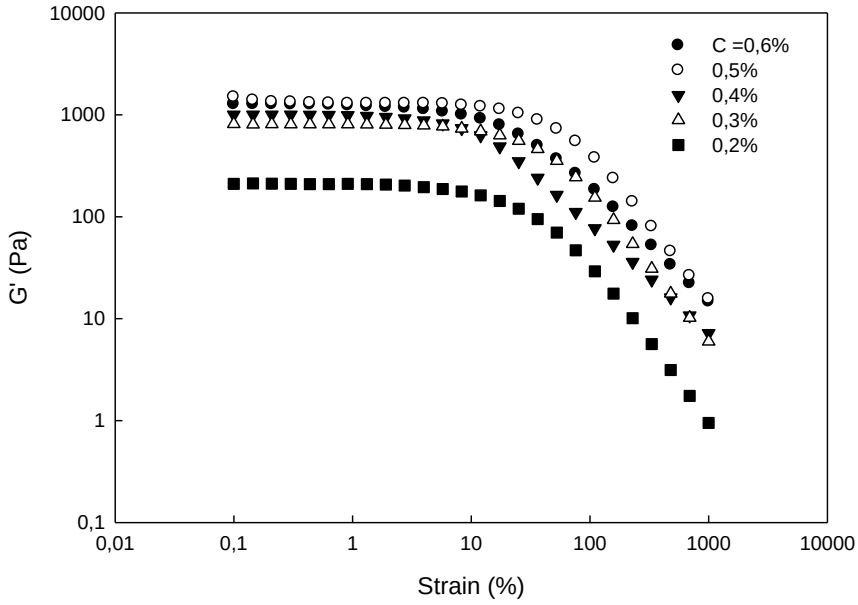

Figure IV.9: Rheological Characterization of the five Hydrogels: Strain Sweep Analyses of Storage Modulus (G').

The strain sweep analysis shows that all samples exhibit a stable storage modulus (G′) in the linear viscoelastic region, followed by a sharp decline beyond a critical strain. The sample at 0.2% concentration displays a significantly lower G′ across the entire strain range, indicating weak network formation and poor mechanical stability. In contrast, the

0.3% formulation presents a much higher and more stable G′, with delayed structural breakdown, suggesting improved gel strength. Therefore, 0.3% was selected as the optimal concentration to balance mechanical integrity and processability.

IV.2.3.2 Flow Curves

The following flow curves were obtained from the apparent viscosity values measured as a function of the variation in shear rate.

Figure IV.12 shows the flow curves of the placebo hydrogels by analysing the variation of viscosity as a function of shear rate.

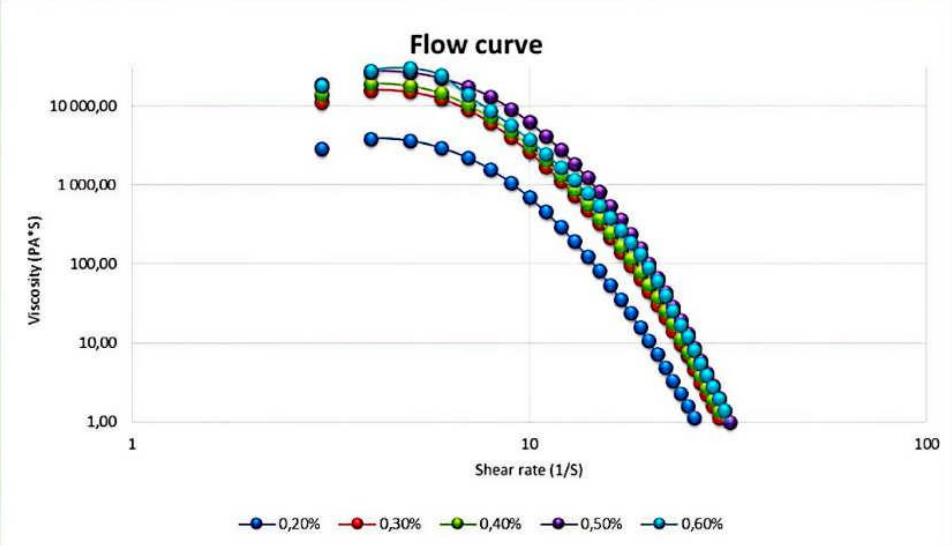

Figure IV.10: Flow curves of placebo hydrogels at different carbopol concentrations.

The curves show a pseudoplastic behaviour of the hydrogels:

Viscosity decreases with increasing shear rate, demonstrating shear-thinning behaviour typical of pseudoplastic materials.

Effect of Carbopol concentration:

- 0.2%: Low viscosity, weakly structured gel network, limited mechanical resistance.
- 0.3%: Moderate viscosity, good balance between consistency, stability, and spreadability.
- 0.4%: Higher viscosity and denser structure, but may show slightly lower mechanical resistance (as seen in viscoelasticity tests).
- 0.5% – 0.6%: Very high viscosity, cohesive and dense structure, but less manageable (less fluid gel).

In conclusion, the 0.3% Carbopol gel demonstrates good and sufficient viscosity for structural stability, while remaining easy to apply. This makes it an optimal choice for pharmaceutical and cosmetic applications

IV.2.4. Spreadability Test:

As shown in Figure IV.13, the spread diameter of the hydrogels increased with the applied weight, confirming that the spread area is proportional to the load with an average area of 37.56 cm².

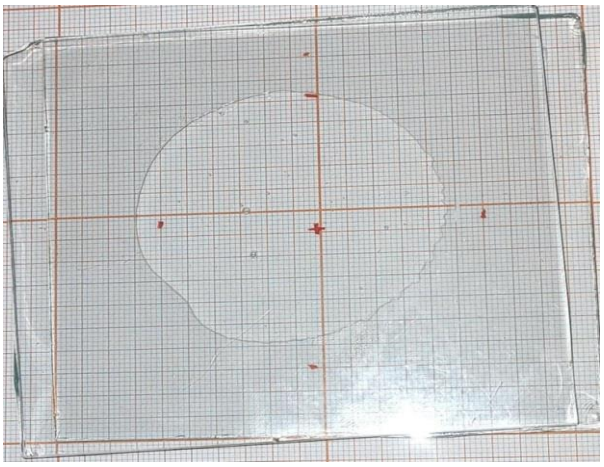

Figure IV.11: Spreadability test on our 0.3% Hydrogel**.**

IV.2.5. Swelling Test:

Bulk hydrogel samples were dried in a hot air oven at 100 °C for 1 hour to ensure thorough dehydration. After cooling, the dried samples were weighed to obtain the initial dry mass ($m_0 \approx 2.850$ g). The samples were then immersed in distilled water at room temperature (~25 °C) to allow rehydration. Swelling was assessed at different time intervals (15, 30, and 60 minutes). At each time point, the hydrogel was removed from the water, gently blotted to remove excess surface moisture, and weighed (mt) to calculate the swelling ratio (TG).

Table IV.3: Swelling test results of the 0.3% hydrogel.

Time (min)	Dry Weight (m_0, g)	Swollen Weight (mt, g)	Swelling Ratio (TG)	Swelling (%)
15	2.850	4.200	0.474	47.4%
30	2.850	4.590	0.610	61.0%
60	2.850	4.970	0.745	74.5%

The swelling ratio increased over time, showing that the hydrogel continues to absorb water. Ideally, the test should be extended until saturation is reached.

IV.2.6. Infrared (IR) Spectroscopy:

The IR spectra of hydrogel are illustrated in the following results:

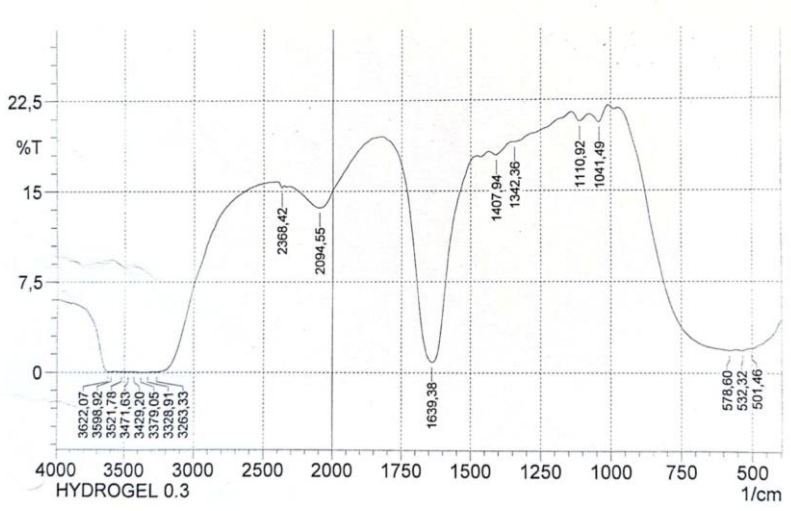

Figure IV.12: FTIR spectra of Hydrogel 0.3%.

The FTIR spectrum of Hydrogel 0.3 exhibits key absorption bands indicative of its chemical structure. A broad band between 3622–3248 cm^{-1} corresponds to O–H stretching vibrations, characteristic of hydroxyl groups and absorbed water.

Peaks at 1639.38 cm^{-1} and 1407.94–1342.36 cm^{-1} are attributed to C=O stretching and symmetric/asymmetric COO^- vibrations, suggesting the presence of carboxylic groups. The bands at 1110.92 and 1041.49 cm^{-1} correspond to C–O–C and C–O stretching, typically found in esters or polysaccharide structures.

Finally, bands in the 578–501 cm^{-1} region may relate to skeletal vibrations of the polymer backbone. These features confirm the hydrogel contains hydroxyl, carboxyl, and ether groups essential for its hydrophilic and functional properties.

IV.3. Characterization of ZnO NPs/Hydrogel:

Once the ZnO nanoparticles were synthesized and the hydrogel was successfully formulated, the next step involved the incorporation of the nanoparticles into the hydrogel matrix, followed by the characterization of the resulting ZnO-loaded hydrogel.

IV.3.1 pH measure:

The initial pH of the ZnO/hydrogel formulation was above 7.5. It was adjusted to 6.5 by adding dilute hydrochloric acid (HCl) to ensure better skin compatibility.

The pH was adjusted to avoid irritating the skin and ensure dermal compatibility.

IV.3.2 Infrared (IR) Spectroscopy:

The IR spectra of hydrogel/ZnO NPs are illustrated in the following results:

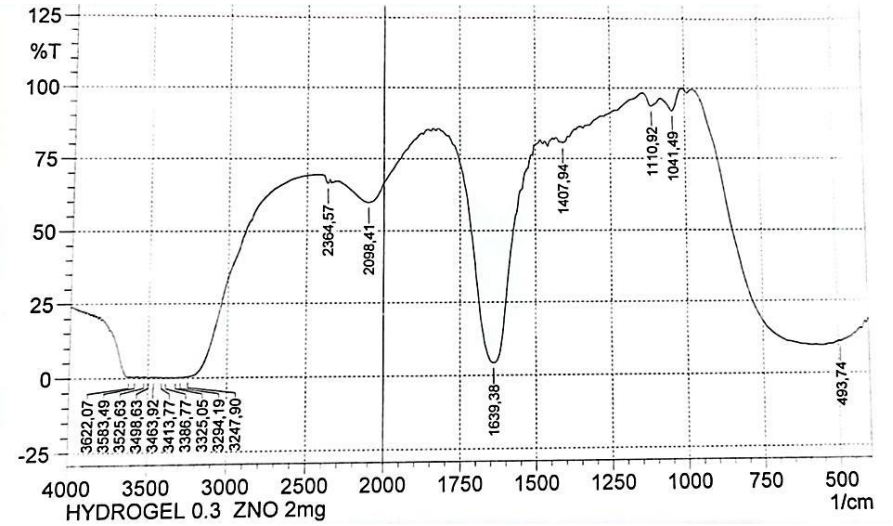

Figure IV.13: FTIR spectra of Hydrogel/ZnO NPs.

The FTIR spectrum of Hydrogel 0.3 loaded with 2 mg of ZnO retains the main functional group signatures observed in the unloaded hydrogel, confirming structural integrity. However, the appearance of a distinct peak at 493.74 cm^{-1} is attributed to ZnO stretching vibrations, providing clear evidence of ZnO nanoparticle incorporation within

the hydrogel network. This modification may enhance the material's functionality, particularly in applications requiring antimicrobial or bioactive properties.

IV.3.3 Rheology study:

IV.3.3.1 Viscoelasticity Test Results:

The following figure presents the viscoelastic properties of hydrogels containing ZnO nanoparticles, by evaluating the variation of G' and G'' as a function of strain and performing a frequency sweep test.

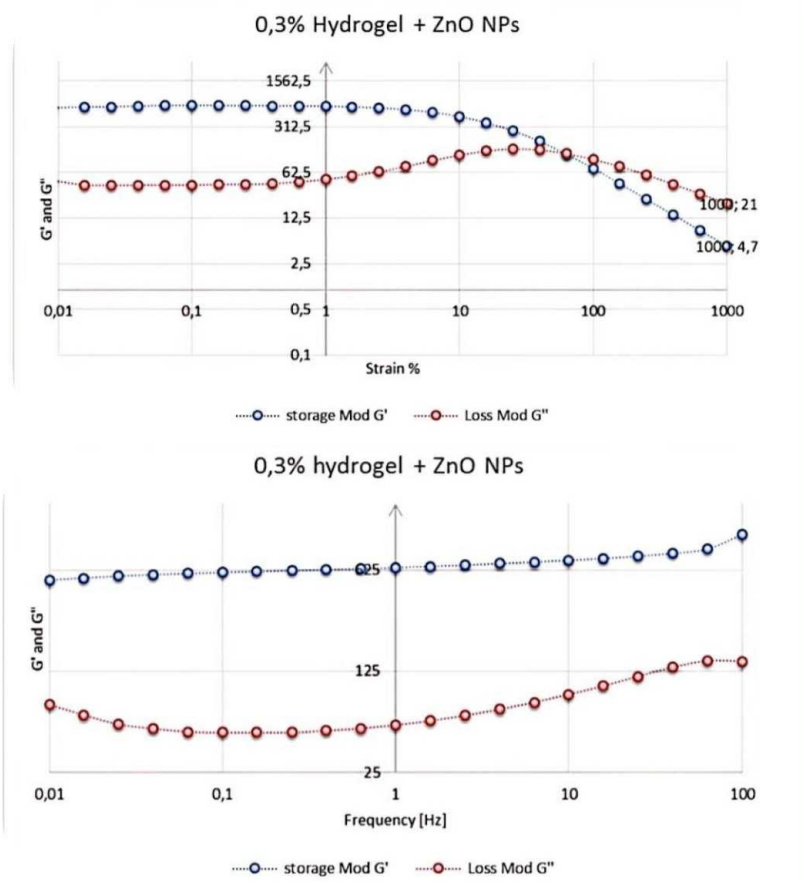

Figure IV.14: Rheological Characterization of 0.3% Hydrogel containing ZnO NPs: Frequency and Strain Sweep Analyses of Storage Modulus (G') and Loss Modulus (G'')

Rheological tests showed that the hydrogel containing 0.3% Carbopol and ZnO nanoparticles exhibits a predominantly elastic behaviour, with the storage modulus (G') being higher than the loss modulus (G'').

- The crossover point between G' and G'' appears at 63.1% strain, indicating good mechanical resistance before the gel structure breaks down.
- The gel remains stable over a wide range of frequencies, with G' > G'' throughout the test, confirming strong structural cohesion.
- The incorporation of ZnO nanoparticles reinforces the polymeric network, enhancing the mechanical stability of the gel.

This favourable viscoelastic behaviour makes the formulation suitable for topical applications, ensuring good consistency, adhesion, and stability.

IV.3.3.2 Flow Curves:

The following figure shows the effect of ZnO NPs incorporation on the behaviour of the prepared hydrogels by studying the variation of viscosity as a function of shear rate (flow curve).

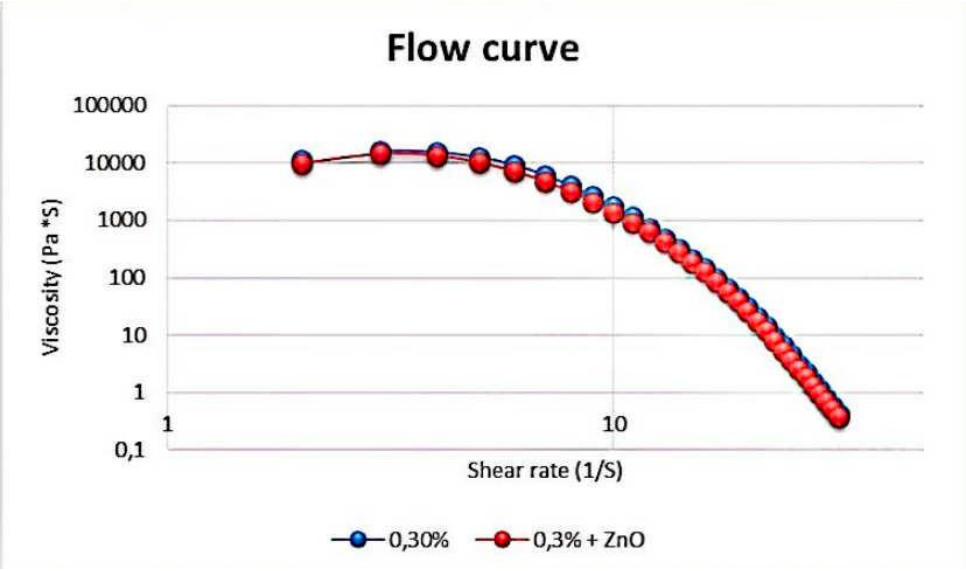

Figure IV.15: Flow curves of hydrogels containing ZnO NPs

The flow curve shows that incorporating ZnO NPs does not significantly affect the shear-thinning behavior of the hydrogel, as the formulation maintain a pseudoplastic profile.

IV.3.4 In vitro study of transdermal diffusion:

IV.3.4.1 Fitting results of the calibration curve of ZnO NPs:

Establishing the calibration curve of ZnO NPs is essential, as it allows us to perform various calculations in order to determine the diffusion parameters.

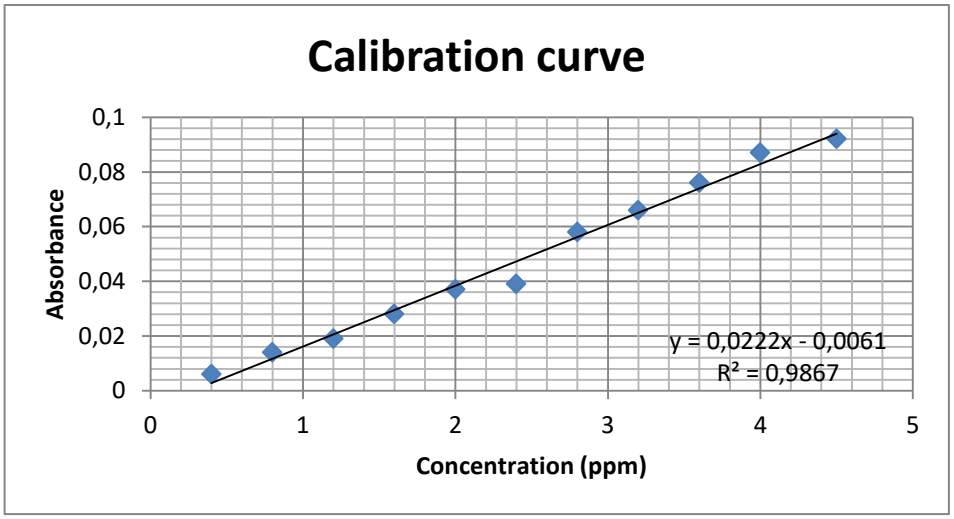

Figure IV.16: Calibration curve of ZnO NPs.

The calibration curve obtained, with the equation $y = 0.0222x - 0.0061$ and a correlation coefficient $R^2 = 0.9867$, was used to determine the concentration of ZnO released from the gel. Based on the measured absorbance values, concentrations were calculated using the linear regression equation (Beer Lambert). The strong linearity of the curve ensures the reliability and accuracy of ZnO quantification in the diffusion medium. This analytical approach effectively supports the evaluation of transdermal release of the active substance.

IV.3.4.2 Study of drug release:

The following figure shows in vitro release of ZnO NPs from hydrogel through synthetic membrane.

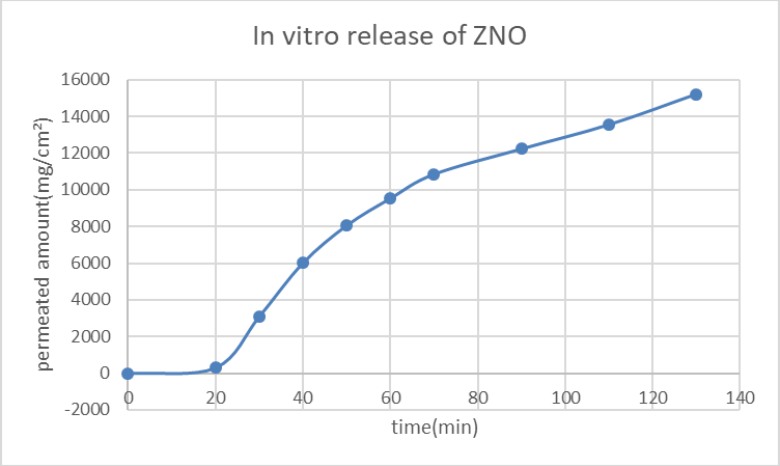

Figure IV.17: in vitro release of ZnO NPs from hydrogel.

The diffusion curve shows a progressive increase in the amount of ZnO NP permeated through the membrane over time, reaching approximately 14,000 ng/cm² at 130 minutes. This indicates a sustained and efficient release of ZnO nanoparticles from the hydrogel matrix.

The release profile showed a gradual increase over time. The diffusion should be monitored to ensure complete drug release and reach saturation.

IV.3.4.3 Kinetic parameters:

The following table shows Key diffusion parameters.

Table IV.4: Key diffusion parameters.

Flux (Jss)	**Permeability coefficient (Kp)**	**Lag time (Tr)**	**Diffusion coefficient (D)**	**Release exponent (n)**
77,351 mg/cm².min	3094,04 Cm/min	17 min	9,8039E-07 Cm²/min	0.9758

• **Flux** (**Jss**): 77.351 mg/cm²·min → Represents the rate at which ZnO permeates through the membrane. This high value indicates a rapid and efficient release, favourable for quick therapeutic action.

• **Permeability coefficient** (**Kp**): 3094.04 cm/min → reflects how easily the ZnO NPs cross the membrane. The high value suggests good permeability of the formulation.

• **Lag time** (**Tr**): 17 minutes → Corresponds to the delay before the start of diffusion. This relatively short lag time indicates that ZnO release begins quickly after application.

• **Diffusion coefficient** (**D**): 9.8039E-7 cm²/min → indicates the ability of ZnO NPs to diffuse through the membrane. This value confirms a controlled and consistent diffusion profile.

• **Release exponent** (**n**): 0.9758 →This value, close to 1, suggests an anomalous (non-Fickian) transport mechanism, involving both diffusion and polymer matrix relaxation. It reflects a controlled and sustained release, suitable for transdermal delivery systems.

IV.3.4.4 Mathematical modelling:

The modelling of transdermal diffusion kinetics was carried out using four different models: zero-order, first-order, Higuchi, and Korsmeyer–Peppas. The fitting of the diffusion profiles to these models are shown below.

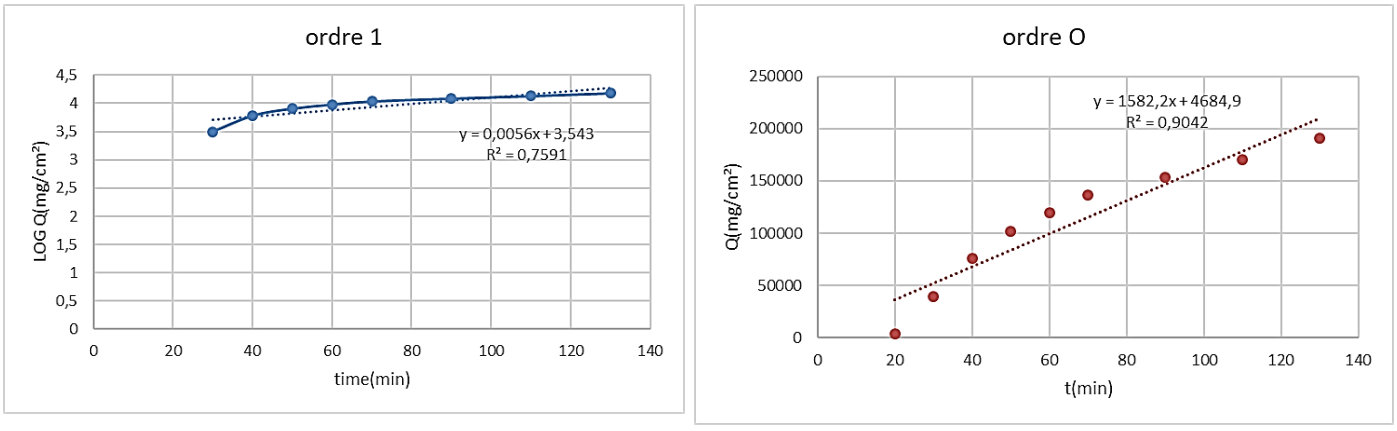

Figure IV.18: Mathematical modelling: order 1 and 0.

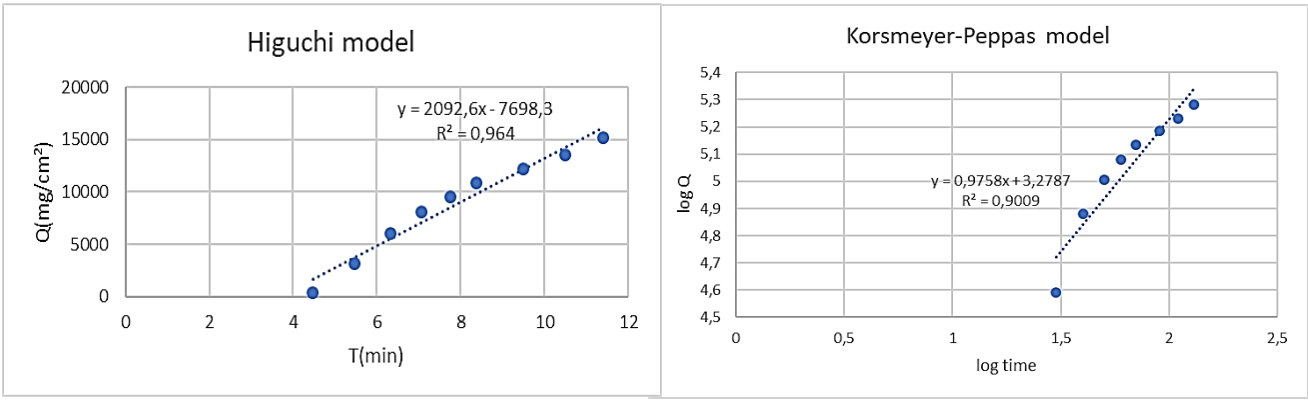

Figure IV.19: Mathematical Modelling: Higuchi and Korsmeyer-Peppas.

The Higuchi model showed the best fit (R^2 = 0.964), indicating that the release of the active compound from the Carbopol-based hydrogel containing ZnO nanoparticles is primarily governed by diffusion through the polymeric matrix.

The Korsmeyer–Peppas model (R^2 = 0.9009) supports a release mechanism close to zero-order, with diffusion being the predominant factor.

The zero-order model (R^2 = 0.9042) suggests an almost constant release rate, consistent with a controlled diffusion system.

The first-order model was less applicable (R^2 = 0.7591), indicating that the release is not directly dependent on the remaining concentration of the active compound.

➢ The diffusion profile of the developed hydrogel is mainly diffusion-controlled, with characteristics close to a zero-order release, making it well suited for sustained transdermal delivery.

IV.3.5 Antimicrobial Activity:

This part of the study reports the outcomes of the antimicrobial evaluation, including both antibacterial and antifungal activity tests.

IV.3.5.1. Antibacterial Activity:

The antibacterial test results are presented in the figures below. Sample 1 corresponds to the hydrogel placebo (without ZnO nanoparticles), sample 2 represents the hydrogel containing 2 mg of ZnO nanoparticles, and sample 3 contains 1 mg of ZnO nanoparticles.

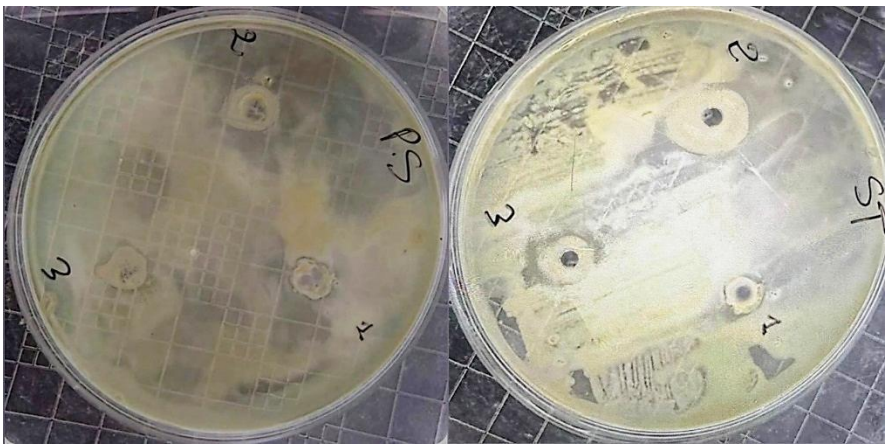

Figure IV.20: Antibacterial Effect of hydrogels/ZnO NPs on PS and ST.

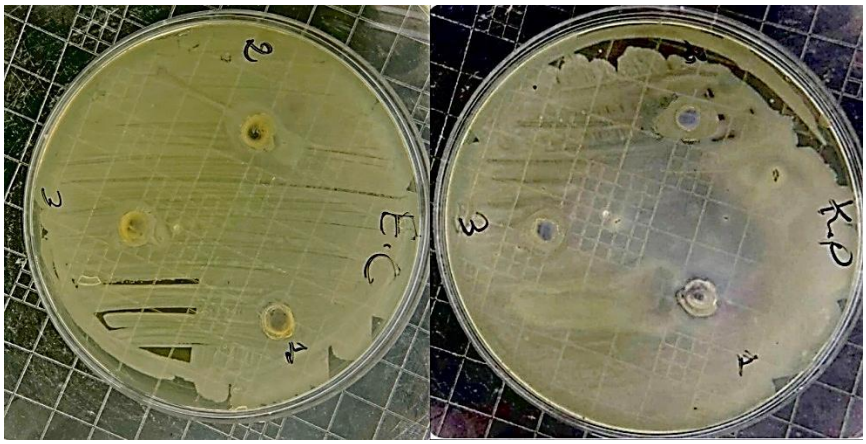

Figure IV.21: Antibacterial Effect of hydrogels/ZnO NPs on KP and EC.

The antibacterial results obtained are illustrated in the table below:

Table IV.4: Antibacterial Activity of the Samples against Different Strains

Strain \ Samples		Hydrogel/ZnO NPs	
		1mg	2mg
Gram négatif	*Pseudomonas aeruginosa*	9	11
	Klensiella pneumonia	7	11
	Escherichia coli	12	20* 12
Gram positif	*Staphylococcus aureus*	13 *14	18

Based on the results presented in the table above, it can be observed that increasing the concentration of ZnO nanoparticles enhances the antibacterial activity against all tested bacterial strains.

The highest antibacterial activity was recorded against the Gram-negative strain *Escherichia coli* and the Gram-positive strain *Staphylococcus aureus*. This suggests a concentration-dependent effect of ZnO nanoparticles, likely due to their increased availability and interaction with bacterial cells at higher doses.

IV.3.5.2. Antifungal Activity:

The antifungal test results shown in the figures below

- ZnO-loaded hydrogel: No antifungal activity observed against Candida albicans.
- ZnO-loaded hydrogel: 12 mm inhibition zone against Candida glabrata, indicating weak antifungal activity.

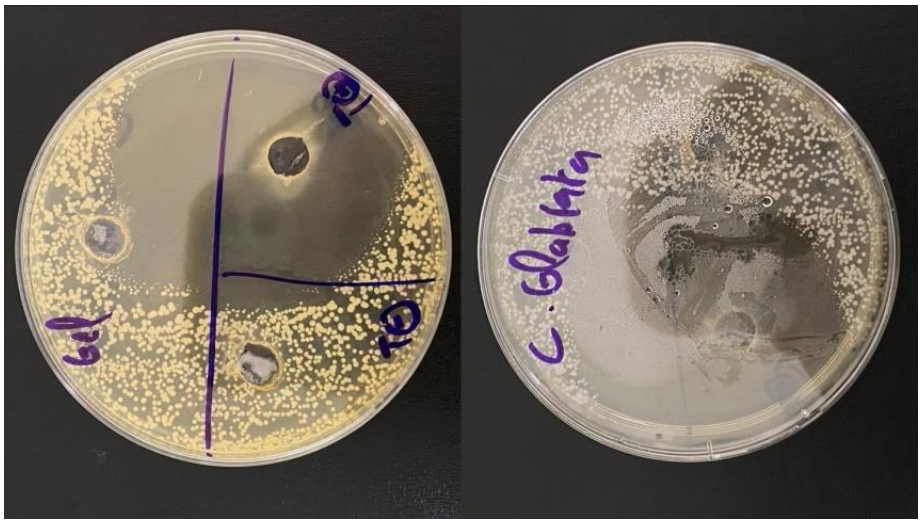

Figure IV.22: Antifungal Activity of Products against Candida Glabrata.

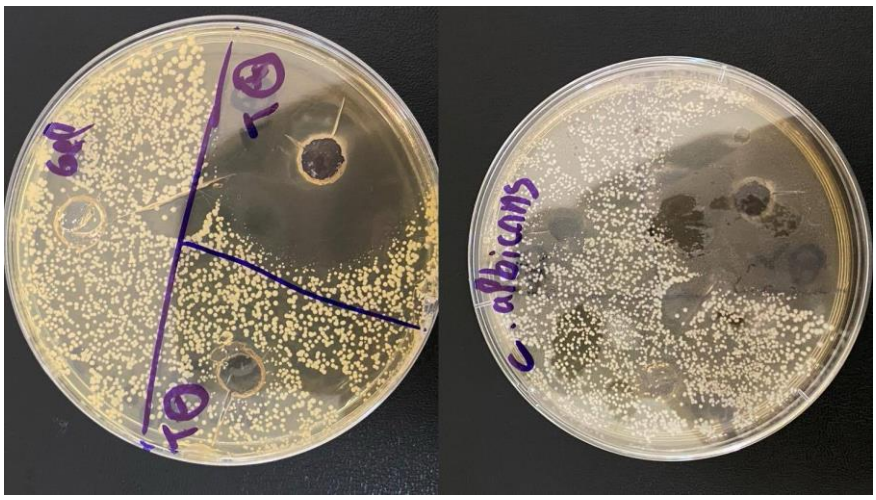

Figure IV.23: Antifungal Effect of Products on Candida Albicans.

The limited antifungal effect observed, especially against *Candida albicans*, could be due to several factors, such as a low concentration of ZnO nanoparticles, limited diffusion of the nanoparticles, or the natural resistance of *Candida glabrata*. Even though the results were not as strong as the positive control (econazole), the inhibition zone observed for *C. glabrata* still suggests that ZnO nanoparticles could be useful as a supportive antifungal agent, especially when included in more advanced drug delivery systems.

The antifungal activity of ZnO nanoparticles is still under investigation and remains less established. Current findings are mostly based on hypotheses and preliminary results.

GENERAL CONCLUSION

GENERAL CONCLUSION:

Nanoparticles incorporated hydrogels with the potential to enhance either mechanical stability or biological performance have gained significant attention in recent years, especially for the delivery of antimicrobial agents. The future prospects of these hydrogels are immense and promising, due to their unique properties such as high water content, biocompatibility, biodegradability, and drug release.

In this study, zinc oxide nanoparticles (ZnO NPs) were successfully synthesized via a chemical precipitation method. The resulting suspension exhibited a characteristic color ranging from white to yellowish-white, indicating the formation of ZnO nanoparticles. Dynamic light scattering (DLS) analysis revealed an average particle size of 6.9 nm, suggesting a narrow size distribution and good colloidal stability.

The synthesized nanoparticles were comprehensively characterized using visual analysis, Fourier-transform infrared spectroscopy (FTIR), UV-Vis spectroscopy, X-ray diffraction (XRD), DLS, and zeta potential measurements. These analyses confirmed the successful formation of ZnO NPs with desirable physicochemical properties suitable for biomedical applications.

Following the synthesis of ZnO nanoparticles, five hydrogel formulations with varying concentrations of Carbopol 940 were prepared. After evaluating their pH and rheological behavior, the formulation containing 0.3% Carbopol was optimized and selected as the most suitable, based on its ideal viscosity and shear-thinning behavior for topical application.

The selected 0.3% Carbopol hydrogel was further characterized. FTIR, pH, spreadability, swelling, and organoleptic tests confirmed its stability and suitability for transdermal delivery.

The ZnO NPs were then incorporated into the hydrogel via in situ formation within the nanoparticle suspension. Post-incorporation analyses including pH measurement, FTIR, rheological characterization, transdermal diffusion testing, and antimicrobial activity assessments demonstrated the successful integration of ZnO NPs into the hydrogel matrix.

The transdermal diffusion study of the ZnO nanoparticle-based hydrogel revealed a controlled release profile, although certain parameters remain to be optimized. These

findings highlight the need for further research to improve the formulation's transdermal efficiency.

The final formulation exhibited promising antibacterial properties, with enhanced activity observed at higher concentrations of ZnO nanoparticles, particularly against *Escherichia coli* and *Staphylococcus aureus,* indicating a concentration-dependent effect. Although no antifungal activity was observed against *Candida albicans*, a 12 mm inhibition zone was recorded against *Candida glabrata*. Additionally, the formulation demonstrated favourable diffusion characteristics through the skin, supporting its potential as an effective transdermal delivery system.

Overall, the findings of this work highlight the potential of ZnO NP-loaded hydrogels as multifunctional platforms for antimicrobial and transdermal therapeutic applications. Future investigations may further optimize the formulation and explore it's in vivo efficacy and safety.

References

References:

[1] Król, A., Pomastowski, P., Rafińska, K., Railean-Plugaru, V., Buszewski, B., "Zinc Oxide Nanoparticles: Synthesis, Antiseptic Activity, and Toxicity Mechanism", *Advances in Colloid and Interface Science*, Vol. 249, (2017), 37–52.

[2] Pasquet, J., Chevalier, Y., Couval, E., Bouvier, D., Bolzinger, M.A., "Zinc Oxide as a New Antimicrobial Preservative of Topical Products: Interactions with Common Formulation Ingredients", *International Journal of Pharmaceutics*, Vol. 479, No. 1, (2015), 88–95.

[3] Sirelkhatim, A., Mahmud, S., Seeni, A., Kaus, N.H.M., Ann, L.C., Bakhori, S.K.M., Hasan, H., Mohamad, D., "Review on Zinc Oxide Nanoparticles: Antibacterial Activity and Toxicity Mechanism", *Nano-Micro Letters*, Vol. 7, No. 3, (2015), 219–242.

[4] Makaoui, N., Moghni, N., Boutemak, K., Akkache, L., Imoudache, H., Hadj-Ziane Zafour, A., "Synergistic Effect of Synthesized ZnO Nanoflowers Coupled with Various Antibiotics Against Pathogenic Microbes: Characterization, Antibacterial and Antifungal Activity Assessment", *Preprint Research Paper*, (2023).

[5] Zahra, S., Bukhari, H., Qaisar, S., Sheikh, A., Amin, A., "Synthesis of Nanosize Zinc Oxide Through Aqueous Sol–Gel Route in Polyol Medium", *BMC Chemistry*, Vol. 16, (2022), 104.

[6] Rania, D., "Synthèse de Nanoparticules d'Oxydes Métalliques et Leur Activité Antibactérienne", *Université Paris-Nord, Paris XIII*, (2019).

[7] Pasquet, J., et al., "Antimicrobial Activity of ZnO Nanoparticles in Topical Formulations", *International Journal of Pharmaceutics*, Vol. 479, No. 1, (2015), 92–95.

[8] Applerot, G., et al., "ZnO Nanoparticle Interactions with Polymer-Based Gels and Their Influence on Drug Delivery", *Biomaterials*, Vol. 32, No. 3, (2020), 1202–1210.

[9] Wang, Z.L., et al., "Size-Dependent Antimicrobial Properties of ZnO Nanoparticles in Gel Formulations", *Nanomedicine*, Vol. 8, No. 5, (2021), 803–815.

[10] Franklin, N.M., et al., "Zinc Oxide Nanoparticles and Their Role in Transdermal Diffusion Enhancement", *Journal of Biomedical Nanotechnology*, Vol. 14, No. 6, (2018), 1012–1025.

[11] Jones, N., et al., "ZnO Nanoparticles in Drug Delivery Gels: Influence on Skin Permeability and Antimicrobial Effects", *Journal of Pharmaceutical Sciences*, Vol. 110, No. 3, (2019), 1056–1063.

References

[12] Taniguchi, N., "On the Basic Concept of Nanotechnology", In *Proceedings of the International Conference on Production Engineering (ICPE)*, Tokyo, Japan, 26–29 August 1974.

[13] Ealia, S.A.M., Saravanakumar, M.P., "A Review on the Classification, Characterisation, Synthesis of Nanoparticles and Their Application", In *IOP Conference Series: Materials Science and Engineering*, IOP Publishing; (2017), p. 3.

[14] Machado, S., Pacheco, J.G., Nouws, H.P.A., Albergaria, J.T., Delerue-Matos, C., "Characterization of Green Zero-Valent Iron Nanoparticles Produced with Tree Leaf Extracts", *Science of the Total Environment*, Vol. 533, (2015), 76–81.

[15] Vassal, M., Rebelo, S., Pereira, M.D.L., *International Journal of Molecular Sciences*, Vol. 22, No. 8061, (2021).

[16] Mekuye, B., Abera, B., *Nano Select*, Vol. 4, (2023), 486–501.

[17] Ealia, S.A.M., Saravanakumar, M.P., "A Review on the Classification, Characterisation, Synthesis of Nanoparticles and Their Application", In *IOP Conference Series: Materials Science and Engineering*, IOP Publishing; (2017), p. 320.

[18] Pan, K., Zhong, Q., "Organic Nanoparticles in Foods: Fabrication, Characterization, and Utilization", *Annual Review of Food Science and Technology*, Vol. 7, (2016), 245–266.

[19] Khan, H.S.Y., Ali Shah, S.Z., Khan, M.N., Shah, A.A., *Catalysts*, Vol. 12, No. 1386, (2022). https://doi.org/10.3390/catal12111386

[20] Bielański, A., *Podstawy Chemii Nieorganicznej*, PWN; (1997).

[21] Makabenta, J.M.V., Nabawy, A., Li, C.-H., Schmidt-Malan, S., Patel, R., Rotello, V.M., "Nanomaterial-Based Therapeutics for Antibiotic-Resistant Bacterial Infections", *Nature Reviews Microbiology*, (2020).

[22] Muzammil, S., Hayat, S., Fakhar, E.A.M., Aslam, B., Siddique, M.H., Nisar, M.A., Saqalein, M., Atif, M., Sarwar, A., Khurshid, A., et al., "Nanoantibiotics: Future Nanotechnologies to Combat Antibiotic Resistance", *Frontiers in Bioscience*, Vol. 10, (2018), 352–374.

References

[23] Da Silva, B.L., Abuçafy, M.P., Berbel Manaia, E., Oshiro Junior, J.A., Chiari-Andréo, B.G., Pietro, R.C.R., Chiavacci, L.A., "Relationship Between Structure and Antimicrobial Activity of Zinc Oxide Nanoparticles: An Overview", *International Journal of Nanomedicine*, Vol. 14, (2019), 9395–9410.

24] Dizaj, S.M., Lotfipour, F., Barzegar-Jalali, M., Zarrintan, M.H., Adibkia, K. *Antimicrobial activity of the metals and metal oxide nanoparticles.* Mater. Sci. Eng. C, vol. 44, pp. 278–284 (2014).

[25] Sánchez-López, E., Gomes, D., Esteruelas, G., Bonilla, L., Lopez-Machado, A.L., Galindo, R., Cano, A., Espina, M., Ettcheto, M., Camins, A., et al. *Metal-Based Nanoparticles as Antimicrobial Agents: An Overview.* Nanomaterials, vol. 10, n° 292 (2020).

[26] Ul Haq, A.N., Nadhman, A., Ullah, I., Mustafa, G., Yasinzai, M., Khan, I. *Synthesis Approaches of Zinc Oxide Nanoparticles: The Dilemma of Ecotoxicity.* J. Nanomater., vol. 2017, Article ID 8510342 (2017).

[27] Canta, M., Cauda, V. *The investigation of the parameters affecting the ZnO nanoparticle cytotoxicity behaviour: A tutorial review.* Biomater. Sci., vol. 8, pp. 6157–6174 (2020).

[28] Da Silva, B.L., Abuçafy, M.P., Berbel Manaia, E., Oshiro Junior, J.A., Chiari-Andréo, B.G., Pietro, R.C.R., Chiavacci, L.A. *Relationship Between Structure and Antimicrobial Activity of Zinc Oxide Nanoparticles: An Overview.* Int. J. Nanomed., vol. 14, pp. 9395–9410 (2019).

[29] Pomastowski, P., Król-Górniak, A., Railean-Plugaru, V., Buszewski, B. *Zinc Oxide Nanocomposites—Extracellular Synthesis, Physicochemical Characterization and Antibacterial Potential.* Materials, vol. 13, n° 4347 (2020).

[30] Wang, Z.L. *Zinc oxide nanostructures: growth, properties and applications.* J. Phys. Condens. Matter, vol. 16, n° 829 (2004).

[31] Kumar, N., Salehiyan, R., Chauke, V., et al. *Top-down synthesis of graphene: a comprehensive review.* FlatChem, vol. 27, n° 100224 (2021).

References

[32] Abid, N., Khan, A.M., Shujait, S., et al. *Synthesis of nanomaterials using various top-down and bottom-up approaches, influencing factors, advantages, and disadvantages: a review*. Adv. Colloid Interface Sci., vol. 300, n° 102597 (2022).

[33] Shaban, A.S., Owda, M.E., Basuoni, M.M., Mousa, M.A., Radwan, A.A., Saleh, A.K. *Punica granatum peel extract mediated green synthesis of zinc oxide nanoparticles: structure and evaluation of their biological applications.* Biomass Convers. Biorefin., vol. 2022, pp. 1–7.

[34] Srivastava, S., Bhargava, A. *Green Nanoparticles: The Future of Nanobiotechnology*. Springer; 2022. p. 1–352.

[35] Singh, L.P., Bhattacharyya, S.K., Kumar, R., et al. *Sol-Gel processing of silica nanoparticles and their applications.* Adv. Colloid Interface Sci., vol. 214, pp. 17–37 (2014).

[36] Newman, S.G., Jensen, K.F. *The role of flow in green chemistry and engineering.* Green Chem., vol. 15, pp. 1456–1472 (2013).

[37] Bokov, D., Turki Jalil, A., Chupradit, S., et al. *Nanomaterial by sol-gel method: synthesis and application.* Adv. Mater. Sci. Eng., vol. 2021, Article ID 1–21 (2021).

[38] Yoshimura, M., Byrappa, K. *Hydrothermal processing of materials: past, present and future*. J. Mater. Sci., vol. 43, pp. 2085–2103 (2008).

[39] Zhu, T., Kang, W., Yang, H., et al. *Advances of microemulsion and its applications for improved oil recovery.* Adv. Colloid Interface Sci., vol. 299, n° 102527 (2022).

[40] Hu, Z., Oskam, G., Searson, P.C. *Preparation and characterization of nanocrystalline ZnO by chemical precipitation.* J. Colloid Interface Sci., vol. 263, pp. 454–460 (2003).

[41] Rodríguez-Páez, J.E., Caballero, A.C., Villegas, M., Moure, C., Durán, P., Fernandez, J.F. *Processing of ZnO and ZnO-based materials.* J. Eur. Ceram. Soc., vol. 21, pp. 925–930 (2001).

References

[42] Singh, S., Gade, J.V., Verma, D.K., Elyor, B., Jain, B. *Exploring ZnO nanoparticles: UV–visible analysis and different size estimation methods.* Opt. Mater., vol. 152, n° 115422 (2024).

[43] Sahu, J., Kumar, S., Ahmed, F., et al. *Electrochemical properties of high-performance supercapacitor based on Nd-doped ZnO nanoparticles and electronic structure investigated with XAS.* SSRN, preprint 4114229 (2022). https://ssrn.com/abstract=4114229

[44] Thanh, N.T.K., Maclean, N., Mahiddine, S. *Mechanisms of nucleation and growth of nanoparticles in solution.* Chem. Rev., vol. 114, n° 15, pp. 7610–7630 (2014).

[45] Khan, A.A., Baig, M.M.F.A., Dhruv, G., Mishra, S., Narayan, R., Gupta, A., Yousif, M. *Zinc oxide nanoparticles: properties, synthesis, and biomedical applications.* Int. J. Nanomed., vol. 17, pp. 3461–3480 (2022).

[46] Wu, J., Zhang, Y., Yan, Y., Li, Y., Liu, X., Wang, J., Tang, J., Liu, J., Zhang, X. *ZnO nanoparticles via hydrothermal and precipitation methods: A comparative study of the properties.* Mater. Chem. Phys., vol. 263, n° 124382 (2021).

[47] Zheng, Y., Li, X., Chen, W. *Recent advances in biomedical applications of zinc oxide nanomaterials.* Curr. Drug Metab., vol. 14, pp. 885–894 (2013).

[48] Sirelkhatim, A., Mahmud, S., Seeni, A., et al. *Review on zinc oxide nanoparticles: antibacterial activity and toxicity mechanism.* Nano-Micro Lett., vol. 7, pp. 219–242 (2015).

[49] Barui, S., Gokhale, J., Goswami, S., et al. *Nano zinc oxide loaded with doxorubicin as a pH-sensitive nanomedicine for breast cancer therapy.* Mater. Sci. Eng. C, vol. 125, n° 112096 (2021).

[50] Padmavathy, N., Vijayaraghavan, R. *Enhanced bioactivity of ZnO nanoparticles—an antimicrobial study.* Sci. Technol. Adv. Mater., vol. 9, n° 035004 (2008).

[51] Murali, M., Yadav, P., Rai, A., et al. *Improved anticancer and antibacterial activity of curcumin using biodegradable nanoparticles.* RSC Adv., vol. 5, pp. 100077–100084 (2015).

[52] Kumar, R., Umar, A., Kumar, G., Nalwa, H.S. *Antimicrobial properties of ZnO nanomaterials: A review.* Ceram. Int., vol. 43, pp. 3940–3961 (2017).

[53] Siddiqi, K.S., ur Rahman, A., Tajuddin, Husen, A. *Properties of zinc oxide nanoparticles and their activity against microbes.* Nanoscale Res. Lett., vol. 13, n° 141 (2018).

[54] Mehmood, A., Baig, M.M.F.A., Khan, A.A., et al. *A review on antimicrobial potential of zinc oxide nanoparticles (ZnO NPs): Mechanism, synthesis, and biomedical applications.* Inorg. Chem. Commun., vol. 143, n° 109920 (2022).

[55] Gunalan, S., Sivaraj, R., Rajendran, V. *Green synthesized ZnO nanoparticles against bacterial and fungal pathogens.* Prog. Nat. Sci. Mater. Int., vol. 22, pp. 693–700 (2012).

[56] Raghupathi, K.R., Koodali, R.T., Manna, A.C. *Size-dependent bacterial growth inhibition and mechanism of antibacterial activity of ZnO nanoparticles.* Langmuir, vol. 27, n° 7, pp. 4020–4028 (2011).

[57] Jones, N., Ray, B., Ranjit, K.T., Manna, A.C. *Antibacterial activity of ZnO nanoparticle suspensions on a broad spectrum of microorganisms.* FEMS Microbiol. Lett., vol. 279, pp. 71–76 (2008).

[58] Azam, A., Ahmed, A.S., Oves, M., Khan, M.S., Memic, A. *Size-dependent antimicrobial properties of ZnO nanoparticles against oral and gastrointestinal pathogenic bacteria.* Int. J. Nanomed., vol. 7, pp. 3747–3755 (2012).

[59] Zhang, L., Jiang, Y., Ding, Y., Povey, M., York, D. *Investigation into the antibacterial behaviour of suspensions of ZnO nanoparticles (ZnO nanofluids).* J. Nanopart. Res., vol. 9, pp. 479–489 (2007).

[60] Emami-Karvani, Z., Chehrazi, P. *Antibacterial activity of ZnO nanoparticle on gram-positive and gram-negative bacteria.* Afr. J. Microbiol. Res., vol. 5, pp. 1368–1373 (2011).

[61] Reddy, K.M., Feris, K., Bell, J., Wingett, D.G., Hanley, C., Punnoose, A. *Selective toxicity of zinc oxide nanoparticles to prokaryotic and eukaryotic systems.* Appl. Phys. Lett., vol. 90, n° 213902 (2007).

[62] Padmavathy, N., Vijayaraghavan, R. *Enhanced bioactivity of ZnO nanoparticles—an antimicrobial study.* Sci. Technol. Adv. Mater., vol. 9, n° 035004 (2008). [Doublon avec réf. 50 – à supprimer ou fusionner]

[63] Brayner, R., Ferrari-Iliou, R., Brivois, N., Djediat, S., Benedetti, M.F., Fiévet, F. *Toxicological impact studies based on Escherichia coli bacteria in ultrafine ZnO nanoparticles colloidal medium.* Nano Lett., vol. 6, pp. 866–870 (2006).

[64] Bian, S.W., Mudunkotuwa, I.A., Rupasinghe, T., Grassian, V.H. *Aggregation and dissolution of 4 nm ZnO nanoparticles in aqueous environments: influence of pH, ionic strength, size, and adsorption of humic acid.* Langmuir, vol. 27, pp. 6059–6068 (2011).

[65] Saptarshi, S.R., Duschl, A., Lopata, A.L. *Interaction of nanoparticles with proteins: relation to bio-reactivity of the nanoparticle.* J. Nanobiotechnol., vol. 11, n° 26 (2013).

[66] Akhtar, M.J., Ahamed, M., Kumar, S., et al. *Zinc oxide nanoparticles selectively induce apoptosis in human cancer cells through reactive oxygen species.* Int. J. Nanomed., vol. 7, pp. 845–857 (2012).

[67] Rasmussen, J.W., Martinez, E., Louka, P., Wingett, D.G. *Zinc oxide nanoparticles for selective destruction of tumor cells and potential for drug delivery applications.* Expert Opin. Drug Deliv., vol. 7, pp. 1063–1077 (2010).

[68] Padmavathy, N., Vijayaraghavan, R. *Enhanced bioactivity of ZnO nanoparticles—an antimicrobial study.* Sci. Technol. Adv. Mater., vol. 9, n° 035004 (2008). [Doublon – même que 50 et 62]

[69] Shinde, S.S., Bhosale, C.H., Rajpure, K.Y. *Oxidative stress and antibacterial activity of ZnO nanoparticles synthesized by using different methods.* J. Appl. Phys., vol. 114, n° 134302 (2013).

[70] Premanathan, M., Karthikeyan, K., Jeyasubramanian, K., Manivannan, G. *Selective toxicity of ZnO nanoparticles toward Gram-positive bacteria and cancer cells by apoptosis through lipid peroxidation.* Nanomedicine, vol. 7, pp. 184–192 (2011).

[71] Hanley, C., Thurber, A., Hanna, C., Punnoose, A., Zhang, J., Wingett, D.G. *The influences of cell type and ZnO nanoparticle size on immune cell cytotoxicity and cytokine induction.* Nanoscale Res. Lett., vol. 4, pp. 1409–1420 (2009).

[72] Sharma, V., Shukla, R.K., Saxena, N., Parmar, D., Das, M., Dhawan, A. *DNA damaging potential of zinc oxide nanoparticles in human epidermal cells.* Toxicol. Lett., vol. 185, pp. 211–218 (2009).

[73] Vandebriel, R.J., De Jong, W.H. *A review of mammalian toxicity of ZnO nanoparticles.* Nanotechnol. Sci. Appl., vol. 5, pp. 61–71 (2012).

[74] Xie, Y., He, Y., Irwin, P.L., Jin, T., Shi, X. *Antibacterial activity and mechanism of action of zinc oxide nanoparticles against Campylobacter jejuni.* Appl. Environ. Microbiol., vol. 77, pp. 2325–2331 (2011).

[75] Kittler, S., Greulich, C., Diendorf, J., Köller, M., Epple, M. *Toxicity of silver nanoparticles increases during storage because of slow dissolution under release of silver ions.* Chem. Mater., vol. 22, pp. 4548–4554 (2010).

[76] ahmad, Naveed, bukhari, Syed Nasir Abbas, hussain, Muhammad Ajaz, ejaz, Hasan, munir, Muhammad Usman, amjad, Muhammad Wahab. "Nanoparticles incorporated hydrogels for delivery of antimicrobial agents: developments and trends", RSC Advances, vol. 14, n° 24, (April 2024), pp. 13535–13564.

[77] Dobrovolskaia, M.A., Germolec, D.R., Weaver, J.L. *Evaluation of nanoparticle immunotoxicity.* Nat. Nanotechnol., vol. 4, pp. 411–414 (2009).

[78] Basnet, P., Inakhunbi Chanu, T., Samanta, D., Chatterjee, S. A review on bio-synthesized zinc oxide nanoparticles using plant extracts: a green approach. *Biocatalysis and Agricultural Biotechnology*; 2018. Volume 15, p. 431–446.

[79] Basnet, P., Inakhunbi Chanu, T., Samanta, D., Chatterjee, S. A review on bio-synthesized zinc oxide nanoparticles using plant extracts: a green approach. *Biocatalysis and Agricultural Biotechnology*; 2018. Volume 15, p. 431–446.

[80] F. Bourdon, « Développement de formes transdermiques à usage hospitalier, à partir de véhicules prêts à l'emploi, pour le traitement des nausées et vomissements chimio-induits », p. 170, 2015.

[81] A. O. Abioye, S. Issah, A. T. Kola-Mustapha, « Ex vivo skin permeation and retention studies on chitosan–ibuprofen–gellan ternary nanogel prepared by in situ ionic gelation technique—a tool for controlled transdermal delivery of ibuprofen », Int. J. Pharm., vol. 490, no 1, p. 112-130, juill. 2015, doi: 10.1016/j.ijpharm.2015.05.030.

References

[82] European Directorate for the Quality of Medicines & HealthCare (EDQM). *European Pharmacopoeia*, 11th ed. Strasbourg: Council of Europe; 2023. Monograph: Zinc Oxide (0431). p. 4025.

[83] https://rbrlifescience.com/streak-plate-method-principal-and-types/